THE JOURNAL OF COMPARATIVE NEUROLOGY 360:413–441 (1995)

Parallel Pathways and Convergence Onto HVc and Adjacent Neostriatum of Adult Zebra Finches (*Taeniopygia guttata*)

ERIC S. FORTUNE AND DANIEL MARGOLIASH
Department of Organismal Biology and Anatomy, University of Chicago, Chicago, Illinois 60637

ABSTRACT

The structure and connectivity of the forebrain nucleus HVc, a site of sensorimotor integration in the song control system of oscine birds, were investigated in adult zebra finches. HVc in males comprises three cytoarchitectonic subdivisions: the commonly recognized central region with large and medium-sized darkly staining cells, a ventral caudomedial region with densely packed small and medium-sized cells, and a dorsolateral region with oblong cells and rows of cells. All three subdivisions project to area X and the robust nucleus of the archistriatum, with more complexity in the classes and distribution of cells than previously reported. In females, HVc is very small and has a cytoarchitecture distinct from that of the three male subdivisions. The structure of HVc in females treated with estradiol at 15 days of age is similar to male HVc.

Tracer studies in males with fluorescent and biotinylated dextrans demonstrate non-topographic projections onto HVc that may carry auditory information, including type 1 and type 2 neurons in subdivisions L1 and L3 of the field L complex, a class of neurons in nucleus interface, nucleus uvaeformis, the caudal neostriatum ventral to HVc, and intrinsic HVc connections. These data are interpreted in terms of HVc's functional properties. Additionally, the neostriatum immediately ventral to HVc receives projections from field L, ventral hyperstriatum, and caudal neostriatum, and projects to a region surrounding RA and near to or into area X. The similarity of the connectivity of HVc and adjacent neostriatum suggests the possibility that they share a common origin.

Indexing terms: songbirds, telencephalon, dorsal ventricular ridge, distributed auditory pathways

HVc[1] is a forebrain nucleus that is part of the song control system in oscine passerine birds (Nottebohm et al., '76). Auditory neurons in HVc have complex properties that result from song learning (Margoliash and Konishi, '85; Volman, '93). In each individual, HVc neurons exhibit response specificity for the temporal and spectral parameters of components of that bird's own learned song, which endows the neurons with selectivity for the bird's own song compared with conspecific songs (Margoliash, '83, '86; Margoliash and Konishi, '85; Margoliash and Fortune, '92). Similar song-selective auditory responses have been observed in other song system nuclei, including the robust nucleus of the archistriatum (RA), area X, the medial nucleus of the dorsolateral thalamus (DLM), and the lateral subdivision of the magnocellular nucleus of the anterior neostriatum (lMAN), but these depend on HVc activity (Doupe and Konishi, '91; Vicario and Yohay, '93). Thus, HVc is a nexus for song selective auditory input to the song system.

Previous studies have been equivocal with respect to sources of auditory input to HVc. On the basis of amino-acid autoradiography and Fink-Heimer degeneration in the canary (*Serinus canarius*), Kelley and Nottebohm ('79) showed that neurons in field L, a thalamorecipient telencephalic auditory area (Karten, '68), did not project directly to HVc but projected to the shelf, a zone adjacent to HVc. This zone was located primarily along the ventromedial borders of HVc, and did not extend along the lateral or rostral borders of HVc. Other studies which used horseradish peroxidase for anterograde and retrograde tract tracing also

Accepted February 7, 1995.

Address reprint requests to Daniel Margoliash, Department of Organismal Biology and Anatomy, University of Chicago, 1025 East 57th Street, Chicago, IL 60637.

[1]HVc is a neostriatal nucleus (Nottebohm, '87) whose original name located it in hyperstriatum ventrale. Here we adopt the acronym as the proper name (see Discussion).

failed to detect a direct projection from the field L complex to HVc (Nottebohm et al., '82; Bottjer et al., '89). To date, auditory input to HVc from the field L complex has been presumed to enter HVc through the shelf, as Katz and Gurney ('81) showed that some neurons in ventral HVc have dendrites that extend into the shelf and caudal neostriatum (NC). These neurons may, therefore, have access to auditory input from field L efferents in the shelf.

Kelley and Nottebohm ('79) also concluded that neurons lateral to field L project directly into HVc. Subsequently, these lateral injections were interpreted by Nottebohm et al. ('82) to have involved nucleus interface (NIf), which was shown to project to HVc via retrograde labeling (Nottebohm et al., '82). Recent cytoarchitectonic data indicate that NIf is partially embedded within field L (Fortune and Margoliash, '92a) suggesting that the lateral injections from Kelley and Nottebohm ('79) may have involved the L1 subdivision of field L. Thus, the projections to HVc seen in the lateral injections of Kelley and Nottebohm ('79) may have arisen from NIf, L1, or both NIf and L1.

HVc may receive additional auditory inputs. Some NIf neurons may have dendrites that ramify extensively within L1 (Fortune and Margoliash, '92a). Uva, a nucleus in the dorsal thalamus which projects to HVc and NIf (Nottebohm et al., '82), also may carry auditory information. Studies of the physiology and connectivity of Uva suggest that this nucleus is multisensory (Okuhata and Nottebohm, '92; Wild, '93), and may be equivalent to the caudal division of the dorsolateral posterior nucleus of the thalamus (cDLP) found in non-oscine species (Wild, '93; also see Gamlin and Cohen, '86; Korzeniewska and Güntürkün, '90). Therefore, NIf, which receives input from Uva, and Uva itself, may be sources of sensory information to HVc, potentially including auditory, visual, and somatosensory modalities.

This report describes the sources and distribution of inputs to HVc. In the first part, we describe the cytoarchitecture of HVc. Although HVc has been the focus of numerous studies, including volumetric studies in relationship to seasonal changes (e.g., Nottebohm, '81; Nottebohm et al., '86; Gahr, '90) and syllable repertoire (e.g., Nottebohm et al., '81; Canady et al., '84; Brenowitz and Arnold, '86; DeVoogd et al., '93), developmental, hormonal, and neurogenesis phenomena (e.g., Bottjer et al., '85; Alvarez-Buylla et al., '92; Kirn et al., '91; Johnson and Bottjer, '93), studies of its cellular constituents (e.g., Nixdorf et al., '89; Watson et al., '88; Braun and Scheich, '88; Braun et al., '91), physiological studies (e.g., Katz and Gurney, '81; Margoliash, '83, '86; Volman, '93), and studies of the connectivity of HVc (e.g., Nottebohm et al., '76; Kelley and Nottebohm, '79; Nottebohm et al., '82; Bottjer et al., '89), a detailed and systematic description of the HVc cytoarchitecture has yet to be obtained. Our description of HVc cytoarchitecture has facilitated the interpretation of injection sites and the resultant patterns of labeling, and should likewise facilitate the interpretation of other results. In particular, we report a new dorsolateral region characterized by large oriented cells and rows of cells, clarify the relationship of the caudomedial region to the rest of HVc, and provide information regarding the discrepancy between the definitions of the shelf based on connectivity (Kelley and Nottebohm, '79) and cytoarchitecture (Nottebohm et al., '82).

The second part of this report describes the results of retrograde and anterograde labeling from injections into HVc, its afferents and efferents, and based on control injections. We have identified the types and distribution of cells in L1 and L3 of the field L complex that apparently project directly into HVc, although a severe fibers-of-passage problem with injections of anterograde tracer prevented final confirmation. We show that some NIf neurons that project to HVc have dendrites that ramify extensively within L1. These neurons may represent a separate class of NIf neurons (Fortune and Margoliash, '92a). None of the afferent projections to HVc, including those from field L, NIf, Uva, and the medial divisions of the magnocellular nucleus of the anterior neostriatum (mMAN; Nottebohm et al., '82) appear to be topographically organized. This massive, non-tonotopic convergence onto HVc can help to explain its complex physiological properties, and its apparently non-topographic functional organization (Margoliash et al., '94).

Our data also have implications for the evolution of the song system. One or more regions in NC adjacent to HVc also receive input from the field L complex, the ventral hyperstriatum (HV), and from other parts of NC. Additionally, NC adjacent to HVc projects to a region adjacent to RA, and to or near area X. Control injections into HV demonstrate a projection from a region adjacent to Uva. Thus, there are similar, multiple parallel pathways that converge onto HVc and onto NC adjacent to HVc, and HVc and NC adjacent to HVc have parallel efferents. The similarity of the connectivity of HVc and immediately adjacent NC gives insight into the evolutionary origins of HVc, and the song system (Margoliash et al., '94).

Some of this work has appeared before in abstract form (Fortune and Margoliash, '92b,c), and has been summarized in a recent review (Margoliash et al., '94).

Abbreviations

A	archistriatum
APH	parahippocampal area
Cb	cerebellum
cDLP	caudal division of dorsolateral posterior nucleus of the thalamus
DA	dorsal archistriatal tract
DVR	dorsal ventricular ridge
HA	accessory hyperstriatum
Hp	hippocampus
HV	ventral hyperstriatum
LAD	dorsal archistriatal lamina
LH	hyperstriatal lamina
lMAN	lateral magnocellular nucleus of the anterior neostriatum
LMD	dorsal medullary lamina
LPO	parolfactory lobe
mMAN	medial magnocellular nucleus of the anterior neostriatum
N	neostriatum
NC	caudal neostriatum
Nd	dorsal neostriatum
NI	intermediate neostriatum
NIf	nucleus interface
OT	optic tectum
Ov	nucleus ovoidalis
P	pineal
PA	paleostriatum augmentatum
PP	paleostriatum primitivum
RA	robust nucleus of the archistriatum
Uva	uvaeform nucleus
X	area X

MATERIALS AND METHODS

Adult male and female zebra finches were obtained from a breeder (Magnolia, CA) and housed in small groups in cages at the University of Chicago. Three male and two female zebra finches were used for Nissl preparations. These birds were given a lethal dose of Nembutal (0.07 cc), perfused transcardially, and their brains removed and stored in 4% w/v paraformaldehyde in saline. The brains were embedded in parlodion (Sigma, St. Louis, MO) and cut on a sliding microtome into 40 μm thick sections. One female and two male brains were cut in the sagittal plane and one male and one female brain were cut in the coronal plane. The sections were stained with cresyl violet and coverslipped with Permount (Sigma). Thirty other male brains and five other female brains, which were obtained in physiological and other experiments, were also examined in this study. These brains were perfused, post-fixed in formal-sucrose, cut on a freezing stage microtome at 40 μm or 50 μm in either the coronal or sagittal plane, and stained with cresyl violet. Additionally, Masakazu Konishi generously provided prepared slides of the brains of six adult females that were administered exogenous 17 β-estradiol (E2) at 15 days of age. These brains were cut using frozen section histology in the sagittal plane and stained with cresyl violet. Cresyl violet histology of the brains of several other species of birds, including male white-throated sparrows (*Zonotrichia albicollis*), eastern meadowlarks (*Sturnella magna*), western meadowlarks (*Sturnella neglecta*), indigo buntings (*Passerina cyanea*), and canaries, which were available in the laboratory, were also examined.

Tracer experiments involved 28 males and two females. Most birds received an injection into each hemisphere. A bird was isolated and deprived of food and water 1 hour prior to surgery. Birds were anesthetized with 0.05 ml Equithesin. The bird's head was immobilized in a custom-made stereotaxic apparatus with ear bars and a beak holder. A fenestra (< 0.5 mm diameter) was opened in the skull at coordinates determined stereotaxically relative to the bifurcation of the mid-sagittal sinus. Injections of 10 mg/ml biotinylated or fluorescent dextrans (Molecular Probes, Eugene, OR) in 0.2 M KCl were made at known depths with a 1 μl syringe (Hamilton model #7001, Reno, NV) using a glass pipette pulled to a tip diameter of approximately 20 μm (Sutter model P-87, Novato, CA) and advanced with a micromanipulator (10 μm resolution). Some injections contained 0.001% v/v Triton X-100 (Sigma). Volumes between 50 nl and 300 nl were ejected over a period of 5 to 15 minutes. The pipette was withdrawn, and the fenestra was covered with acrylic cement. The bird was returned to the aviary after it recovered from anesthesia.

The bird was maintained for a period of 36 to 72 hours, with shorter survival times favoring anterograde labeling and longer survival times favoring retrograde labeling. At the end of this period the bird was given a lethal dose of Nembutal. When deep anesthesia was achieved, the bird was perfused transcardially, first with 0.9% NaCl w/v 0.1 M phosphate buffer solution (PBS), and then with 4% paraformaldehyde w/v PBS. The brain was removed and stored at 4°C for 5 to 12 hours in the paraformaldehyde solution with 10% w/v sucrose. The brain was cut in either coronal or sagittal planes on a freezing stage sliding microtome at a thickness of 50 μm. Sections with fluorescent dextrans were mounted on slides and coverslipped with 1% v/v n-propyl gallate (Sigma) in glycerol. The sections with biotinylated dextrans were collected in PBS and transferred into an avidin-peroxidase solution (Vector Laboratories, Burlingame, CA). Sections remained in the avidin-peroxidase solution for up to 6 hours (2 hours minimum) at room temperature. They were then rinsed in PBS followed by distilled water, mounted on gelatin coated slides, and allowed to dry on the slides at room temperature. The slides were rinsed in PBS, transferred into a solution of 1 mg/ml diaminobenzidine (DAB; Sigma) in PBS for 15 minutes, and then moved into 0.1% hydrogen peroxide in PBS. In most cases the DAB solution contained an enhancing agent (< 1 mg/ml filtered CoCl). The reaction was visually monitored for background staining. Reactions typically lasted between 2 to 5 minutes. After reaction, the slides were rinsed several times in PBS. The sections were then dehydrated in alcohol, immersed in xylenes, and coverslipped with Permount.

Nissl sections were analyzed and drawn using a Zeiss Standard GFL microscope fitted with a camera lucida drawing tube. High power photomicrographs were taken on a Zeiss Axioplan. The Zeiss Axioplan also had Nomarski attachments, which was used for examination of fibers and unstained material. Fluorescent material was viewed and photographed with a Nikon Optiphot-2.

RESULTS

The results are presented in three major sections. The first section describes the cytoarchitecture of HVc in adult males, adult females, and adult females treated with E2 as juveniles. The second section describes injections of HVc efferent targets, RA and area X, and injections into HVc itself, to determine the distribution of efferent cells within HVc. The third section describes injections into HVc and other structures which show the pattern of afferents to HVc and to adjacent neostriatum.

Cytoarchitecture of HVc

HVc in male zebra finches is a ridge on the dorsal and dorsomedial surface of caudal dorsal ventricular ridge (DVR) (Fig. 1). In brains fixed with glutaraldehyde – where the tissue shrinks considerably, HVc is visible through the parahippocampus (APH). In brains which are formalin fixed, or *in vivo* (Fortune and Margoliash, '94), HVc is often not visible through APH, though it can be seen once APH has been dissected away (Fig. 1). The size and height of this ridge varies between birds. The lateral edge of HVc is between 350 μm and 650 μm rostral to the medial pole. Figure 1 shows the locations of the sections from Figures 3 and 5. Female HVc is in the same relative position as male HVc, but does not form a ridge on the surface of DVR. HVc of both males and females appears in Nissl sections as a dark region on the dorsal edge of the caudal neostriatum that lies along the ventricle (Figs. 2–6).

The shelf is a fiber-rich zone which forms most of the ventral border of HVc in males and the entire ventral border of HVc in females. In males, the shelf is most distinct around rostrolateral HVc and does not extend around the caudomedial borders of HVc. Thus, the shelf helps to demarcate the ventral border of central HVc but not of caudoventral HVc (see Discussion). The caudomedial borders of male HVc, where the shelf is absent, are not distinct. In males the shelf contains fibers that are oriented in sagittal axis. Fibers in the shelf of females do not appear to be oriented.

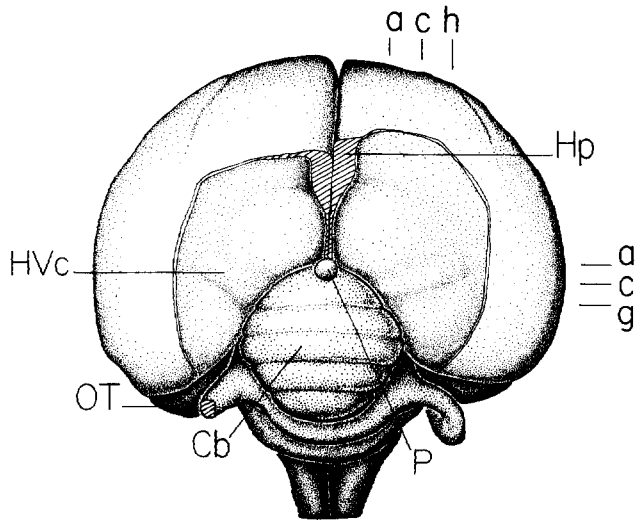

Fig. 1. Dorsal view of male zebra finch brain with parahippocampus, dorsal cortex, and part of the hippocampus removed. HVc appears as a ridge extending across DVR from where the cerebellum contacts DVR to approximately 2.5 mm lateral to the midline. The size and shape of this ridge varies between birds, which probably reflects a combination of natural variation and differences in shrinkage during fixation. The lines at the edges of the brain indicate the levels of sections in Figures 3 (side) and 5 (top). Letters correspond to the respective panels in each of those figures.

Definition of male HVc in Nissl stained sections

Three cytoarchitectonic subdivisions of HVc are recognized in male zebra finches. Central HVc, which forms the bulk of the nucleus, has large clusters of large and medium-sized darkly staining cells. A second region, in ventral caudomedial HVc (the 'caudomedial region'), contains smaller and more densely packed cells and cell clusters than does the rest of HVc. The third subdivision is a zone of large, oblong cells that appear oriented parallel to the ventricle. These cells are arranged in rows of cells in the rostral-caudal plane, and as a result are best seen in parasagittal material. We have also examined Nissl material of male white-throated sparrows, eastern meadowlarks, western meadowlarks, indigo buntings, and canaries. In all five species the three cytoarchitectonically defined subdivisions of HVc are also present, although there are distinct differences in the structure of HVc between these species whose description is beyond the scope of this report.

Coronal sections

In coronal sections, the apparent location, shape, and cytoarchitecture of HVc progressively changes along the rostrocaudal axis of the brain (Fig. 2). In the most caudal sections, where the cerebellum is present, HVc lies along the dorsomedial edge of DVR. In these sections HVc is a dark wedge with clear spots or vertical stripes that are rich with fibers (Figs. 2e, 3a). The lateral end of HVc is thicker than the medial end, which forms a point along the medial edge of DVR. Typically, the ventral border of HVc in caudal sections is distinct. The fiber-rich zones in dorsal HVc (along the ventricle), and ventral to HVc (the shelf), are not seen in these sections. Caudal HVc is composed of large and medium-sized clusters of darkly staining cells (Fig. 3a,b). These clusters are similar to those in most of HVc, except that the cells in the clusters appear to be more densely packed. The dense packing of these clusters gives them the appearance of large cells in photomicrographs (e.g., Fig. 3b and 3e,f), but a closer examination reveals several cells and their individual nuclei of different size. Caudal HVc often appears somewhat darker than the rest of HVc.

In more rostral sections HVc has its greatest mediolateral length (~ 1.5 mm) and extends across the medial and dorsal edges of the caudal neostriatum (Figs. 2c, 3c). Medially, HVc extends ventrally to a point along the medial edge of DVR. The ventral border of medial HVc is often not distinct medially. Laterally, HVc contains large, widely spaced clusters of large and medium-sized cells which are darkly staining (Fig. 3e), whereas medially HVc has small and medium-sized cells and cell clusters that are less darkly staining (Fig. 3d). The medial and lateral parts of HVc appear to be equally dark at low power magnification. The lateral region has a grainy appearance due to the widely spaced dark clusters, whereas the medial region does not. The lateral region is also demarcated by the presence of a 10 to 25 μm thick cell-poor zone along the ventricle. Moving from lateral to medial, the density of cells and cell clusters increases and the proportion of large dark clusters decreases gradually. There is, however, no distinct border between the medial and lateral regions although the transition between cell types often occurs at roughly the same location where the shelf fades medially (Figs. 2c, 3c). Frequently there are blood vessels in the shelf or just dorsal to the shelf in this transition area. Occasionally these vessels cross the entire dorsoventral extent of HVc (e.g., Fig. 2c).

In the most rostral sections, HVc flattens and moves laterally, away from the medial border of DVR. This lateral movement is exaggerated by two factors. First, the medial border of DVR bulges medially rostral to the cerebellum (see Figs. 1, 2). The expansion includes the field L complex and adjacent neostriatum (Fortune and Margoliash, '92a). Second, the caudomedial region, which appears along the medial and ventromedial edge of HVc in more caudal sections, shrinks and disappears rostrally. Rostral HVc has a smaller mediolateral length than in more caudal sections, which is a result of the disappearance of the caudomedial region in rostral HVc. At these levels HVc is disc shaped, with a mediolateral length of less than 1 mm and a thickness of less than 0.5 mm (Figs. 2a, 3g). In rostral sections some cells in the middle of HVc are oriented (Fig. 3f). The shelf is thick and distinct around rostral HVc and surrounds the entire ventral border of HVc (Figs. 2a,b, 3g).

The cells in rostral HVc are generally large and darkly staining (e.g. Fig. 3f,i). Dorsally there is a thin fiber-rich strip directly adjacent to the ventricle which has very few oblong cells in it. Below this fibrous strip there is a zone of large, dark cells which are also oblong or ovoid in shape (Fig. 3i). This zone of cells is present only in dorsal HVc, and is better visualized in parasagittal sections. There are also oblong cells in HVc which lie along the shelf. The cells in the shelf, which are generally small, are also oblong or flattened, and oriented parallel to the shelf (Fig. 3h). The orientation of cells in the shelf is better seen in parasagittal sections.

Parasagittal sections

In most respects, the descriptions of male HVc in coronal and sagittal material are similar (Fig. 5, cf. Fig. 3). This

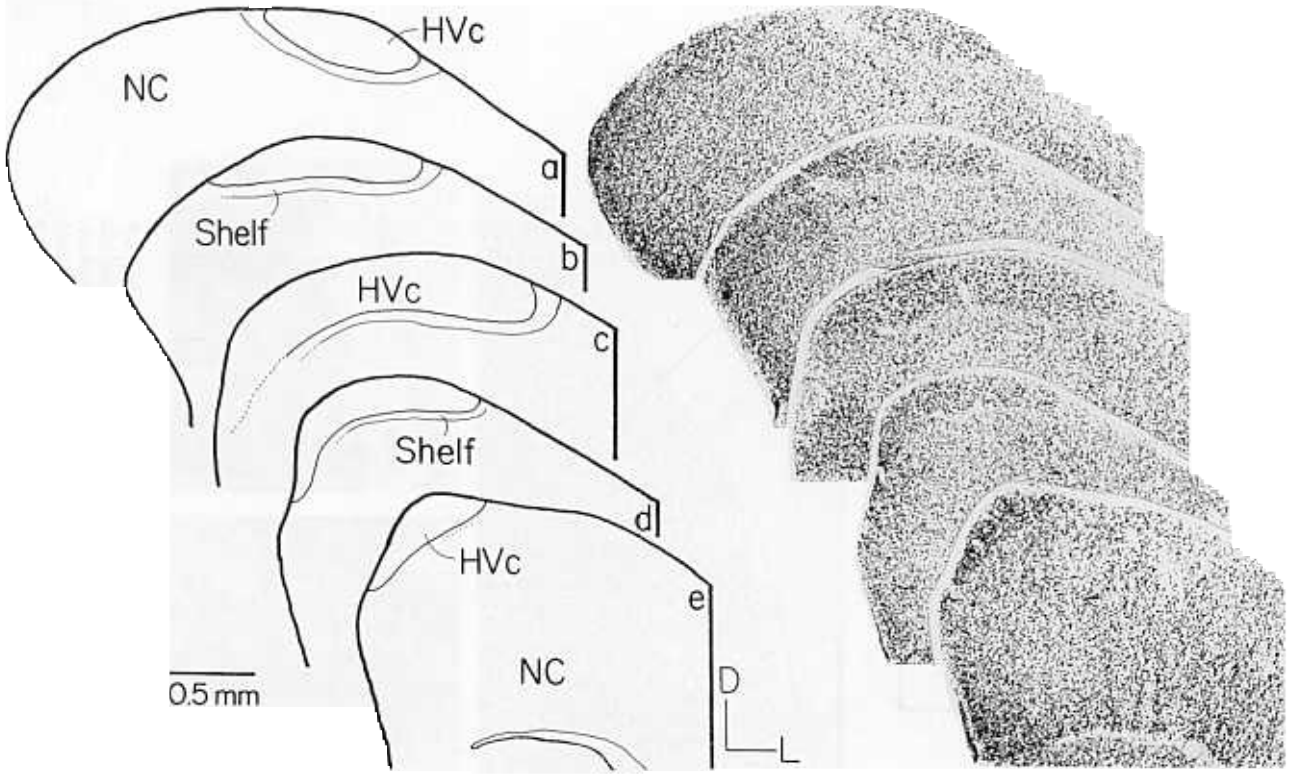

Fig. 2. Coronal sections through male HVc. Line drawings on the left correspond to the photomicrographs on the right. (a) is the most rostral section and (e) the most caudal. Central HVc is present in all five sections. The dorsolateral zone is not distinct in these photographs, but is present in (a). The caudomedial area is in (c) and (d). The shelf is most distinct in (a), and progressively shrinks caudally.

obtains, in part, because the caudal pole of HVc is medial, and the rostral pole is lateral. HVc in caudal coronal sections appears similar to HVc in medial parasagittal sections, and HVc in rostral coronal sections is similar to HVc in lateral parasagittal sections. Coronal and parasagittal sections through the middle of HVc differ in appearance, but contain the same subdivisions. The caudomedial region, which is easily distinguished in coronal material, is not clear in parasagittal material. Lateral HVc is often embedded in bundles of LH fibers that break off from the lamina. As a result, the exact lateral borders of HVc are difficult to determine in parasagittal material, and the shelf is not always recognizable (e.g., Fig. 4e).

The oriented cells in dorsolateral HVc that appear in lateral parasagittal material are not easily seen in coronal material. In lateral parasagittal material, HVc forms a large oval and approaches LH (Fig. 4d,e). At these levels bundles of fibers leave LH, crossing the neostriatum to the rostral edge of HVc (Figs. 4d,e, 5h). Dorsally, there is a thin (20–50 μm) fibrous strip along the ventricle which contains very few cells and extends both rostral and caudal of HVc (Fig. 5g,h). Nomarski microscopy reveals that there are fibers in this zone and that they run in a rostrocaudal orientation. Ventral to the fiber strip in dorsal HVc are large ovoid cells that are oriented parallel to the ventricle (Fig. 5g,h). These cells form rows of several cells in a zone up to 300 μm thick, and the rows are also parallel to the ventricle. Ventral to this zone, HVc has large clusters of large and medium-size darkly staining cells (Fig. 5h,j). The entire ventral border of HVc is demarcated by the shelf. The shelf contains small and medium-sized oblong cells that are oriented parallel to the shelf (Fig. 5i). Fibers in the shelf appear to run rostrocaudally as seen under Nomarski microscopy. In many birds, we see cell-poor streaks which start within central or caudal HVc and, running parallel to the ventricle, exit HVc caudally to enter DA. These streaks are bundles of fibers, which can be seen in Nomarski microscopy and are labeled by injections of tracers into RA (Fig. 13a) or into HVc. In some parasagittal cases we also observed a region caudal to HVc which has a low density of small, fusiform cells (Fig. 5f). We have been unable to identify a corresponding region in coronal sections.

Definition of female HVc in Nissl stained sections

Female HVc is in approximately the same position as male HVc, though it is much smaller, does not contain the same cell types seen in male HVc, and does not form a ridge on the dorsomedial surface of DVR. In general, female HVc is not distinct, and can be difficult to locate, especially in coronal sections. In parasagittal sections, HVc is usually a small, thin (< 200 μm) dark band about 1 mm caudal to LH (Fig. 6a). Although HVc may not be darker than the surrounding neostriatum, the cells in HVc are darkly staining, and appear larger than the cells in the adjacent neostriatum (Fig. 6a,b). Along the ventral border of HVc, there is a thin cell poor zone. Nomarski microscopy of this zone does not reveal oriented fibers. The individual cell clusters in female HVc are not as tightly packed as the clusters in male HVc.

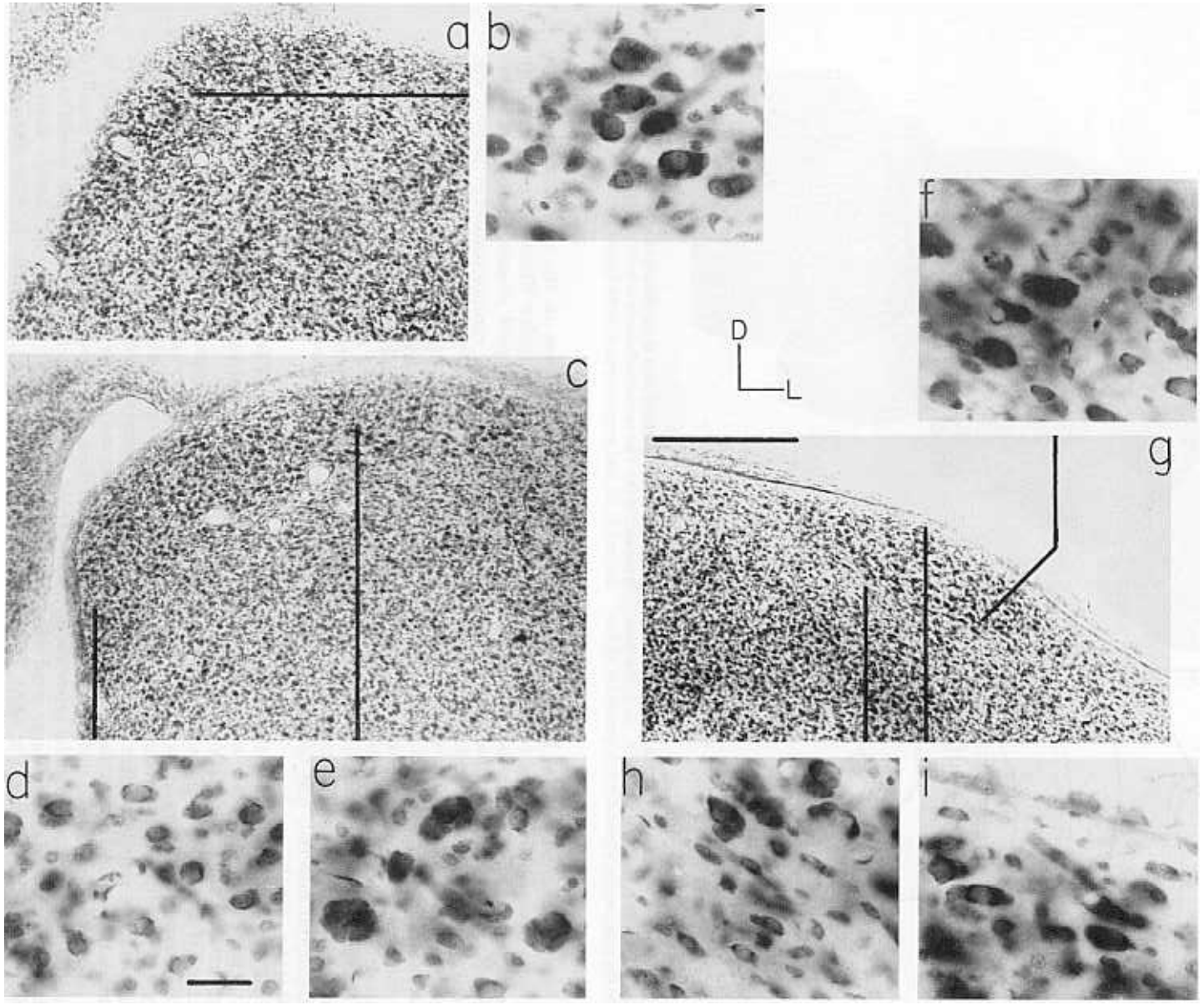

Fig. 3. Coronal sections and high power (40× objective) photomicrographs of male HVc. In this and Figures 5 and 6, all the low power photomicrographs share the same magnification, as do all the high power photomicrographs. Lines in a, c, and g indicate the location of the cells shown in the high power photomicrographs. **a:** Caudal HVc. HVc is the dark region at the dorsomedial corner of DVR along the ventricle. There are clear streaks and holes which contain axons. **b:** Densely packed clusters of cells in caudal HVc. **c:** Middle of HVc. This section contains both the caudomedial (d) and central (e) regions. **d:** Caudomedial region, characterized by small and medium-sized cells and cell clusters. **e:** Central region, characterized by large, darkly staining cells and clusters of cells. **f:** Rostrally, some cells in the central region are oriented parallel to the shelf. **g:** Rostral HVc. This section contains both central HVc and the dorsolateral zone. **h:** The shelf, which contains small, oblong cells. **i:** Dorsolateral zone with large and medium-sized oblong cells. The scale bar in g indicates 500 μm and in d indicates 20 μm.

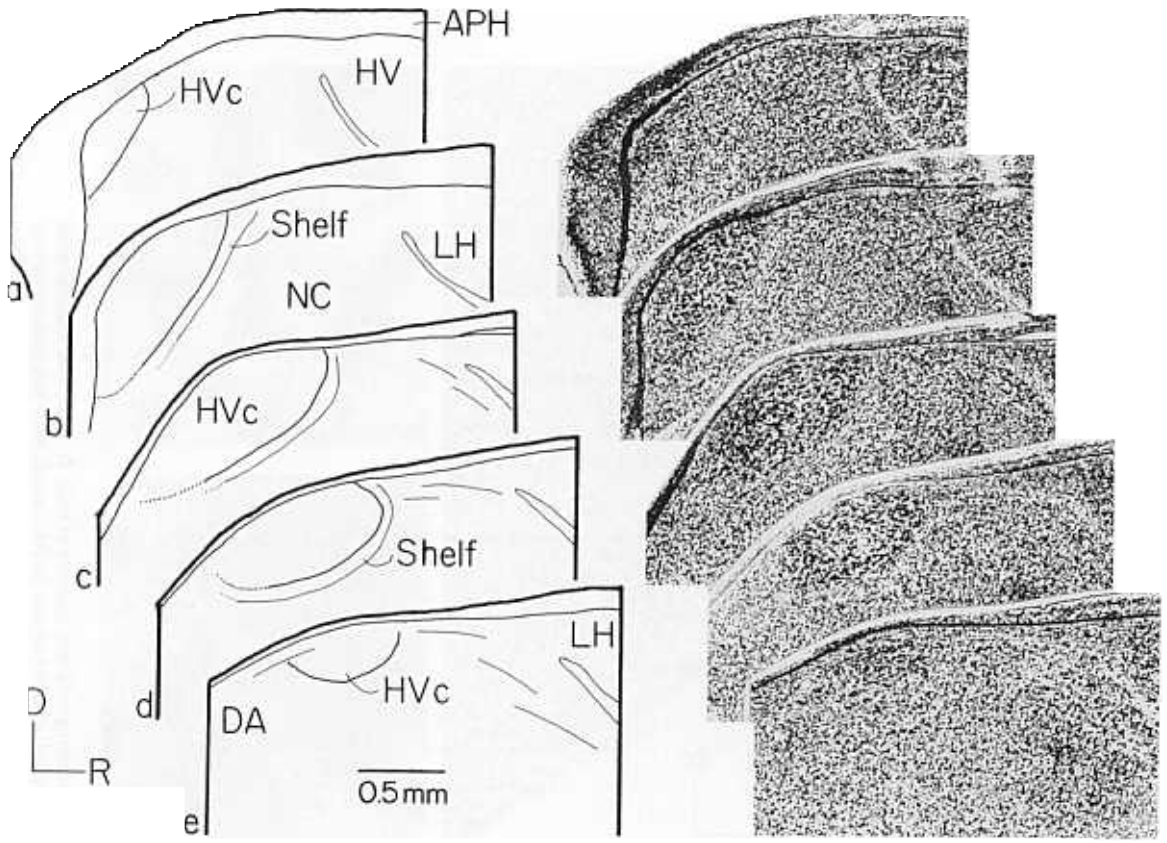

Fig. 4. Parasagittal sections through male HVc. (a) is the most medial section and (e) is the most lateral section. Central HVc is present in all five sections. The dorsolateral zone is distinct in (d), and is also present in (c) and (e). The caudomedial area is present in (a–c). The shelf is distinct in (b–d).

In contrast, the HVc of females that were treated with E2 on day 15 have an appearance similar to that of male HVc (Fig. 6c,f). In these females all three cytoarchitectonic regions found in males can be recognized. The dorsolateral zone is the least developed subdivision, with few oriented cells and clusters of cells (Fig. 6d). The caudomedial region of E2 females is similar to males, having small and medium-sized cells and cell clusters (Fig. 6e). As in males, the border between the caudomedial and central regions is not distinct. The central region contains large clusters of large and medium-sized cells that are darkly staining (Fig. 6g). The central region of these E2-treated females is not distinguishable from the central region of males.

Definition of HVc in retrograde material

Projection of HVc onto area X. Injections of fluorescent dextrans (two cases) and biotinylated dextrans (three cases) into area X in males labeled cells throughout HVc (Fig. 7). These injection sites were large, including a large part of area X and some adjacent tissue. Retrogradely labeled cells were found throughout all three subdivisions of HVc and in the neostriatum ventral to HVc (Fig. 8). There were no apparent differences in the density of cells in each of the three subdivisions of HVc, whereas the density of labeled cells in NC was considerably lower than that in HVc. Because all of our injections into area X included at least some of the surrounding LPO, we could not determine whether the cells labeled in NC project into or around area X.

In males, most cells labeled by injections into area X have medium-sized somata (10–15 μm diameter). Some of these cells were well-filled and had a morphology similar to that of thick dendrite (TD) cells defined in Golgi material (Nixdorf et al., '89), including spiny, medium-diameter (~1–2 μm) dendrites. TD cells had roughly spherical dendritic arborizations (Fig. 7b), similar to TD_1 cells, or elongated arborizations (Fig. 7a), similar to TD_2 cells (Nixdorf et al., '89). In addition, we observed labeled cells with small somata (8–10 μm diameter). In well-filled examples, these cells had large (150 μm diameter) dendritic arborizations, and thin dendrites (~1–2 μm diameter) covered with a moderate density of spines. These cells do not correspond to any of the three morphological classes of cells described in Nixdorf et al. ('89). Additionally, some X-projecting cells had small dendritic arborizations, and were similar in appearance to short dendrite (SD) cells shown in Nixdorf et al. ('89). These cells cannot be conclusively be identified as SD, because they may be poorly filled examples of the cell type shown in Figure 9. For all classes of X-projecting cells there were well-filled examples of cells near the ventral border of HVc that had dendrites that extended ventrally out of HVc (e.g., Fig. 7a,c). In two females, injections of retrograde tracer into LPO labeled a very few (<10) cells in HVc (Fig. 10). These cells had somata of 10-15 μm. The cells in female HVc were not well filled, and therefore could not be classified.

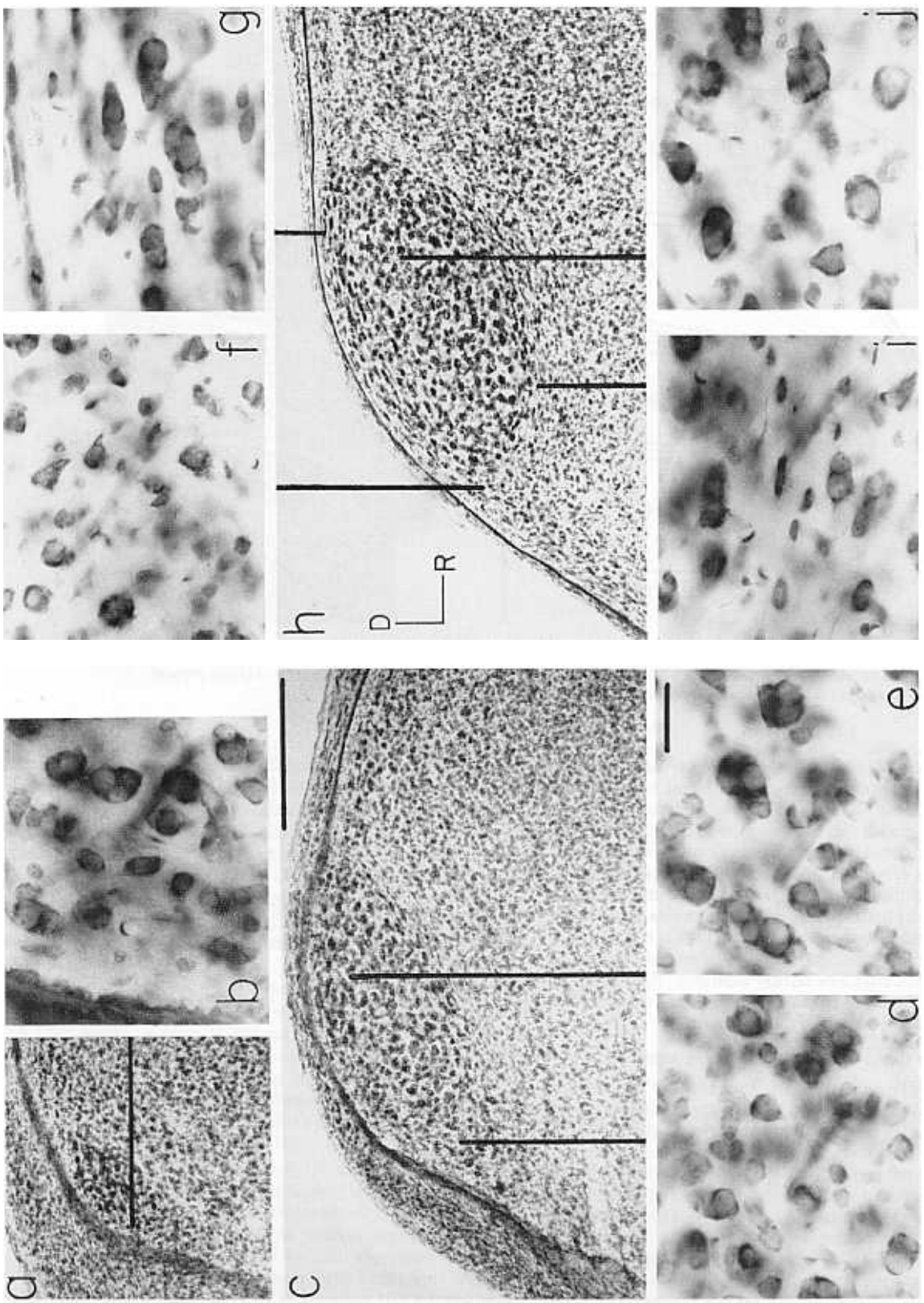

Fig. 5. Parasagittal sections and high power (40× objective) photomicrographs of male HVc. Lines in a, c, and h indicate the locations of the cells shown in the high power photomicrographs. **a:** HVc (central region) is the dark region at the dorsocaudal edge of DVR. **b:** Densely packed clusters of cells in medial HVc. This section contains both the caudomedial (d) and central (e) regions. **d:** Caudomedial region of HVc, characterized by small and medium-sized cells and cell clusters. **e:** Central region of male HVc, characterized by large, darkly staining cells and clusters of cells. **f:** Small and medium-sized cells and cell clusters caudal to HVc which were not seen in coronal material. **g:** Dorsolateral zone of male HVc with large and medium-sized oblong cells that are often in rows. **h:** Lateral HVc. This section contains the central and dorsolateral regions. **i:** The shelf. **j:** Central region—similar to e. Scale bar in c indicates 500 μm and the scale bar in e indicates 20 μm.

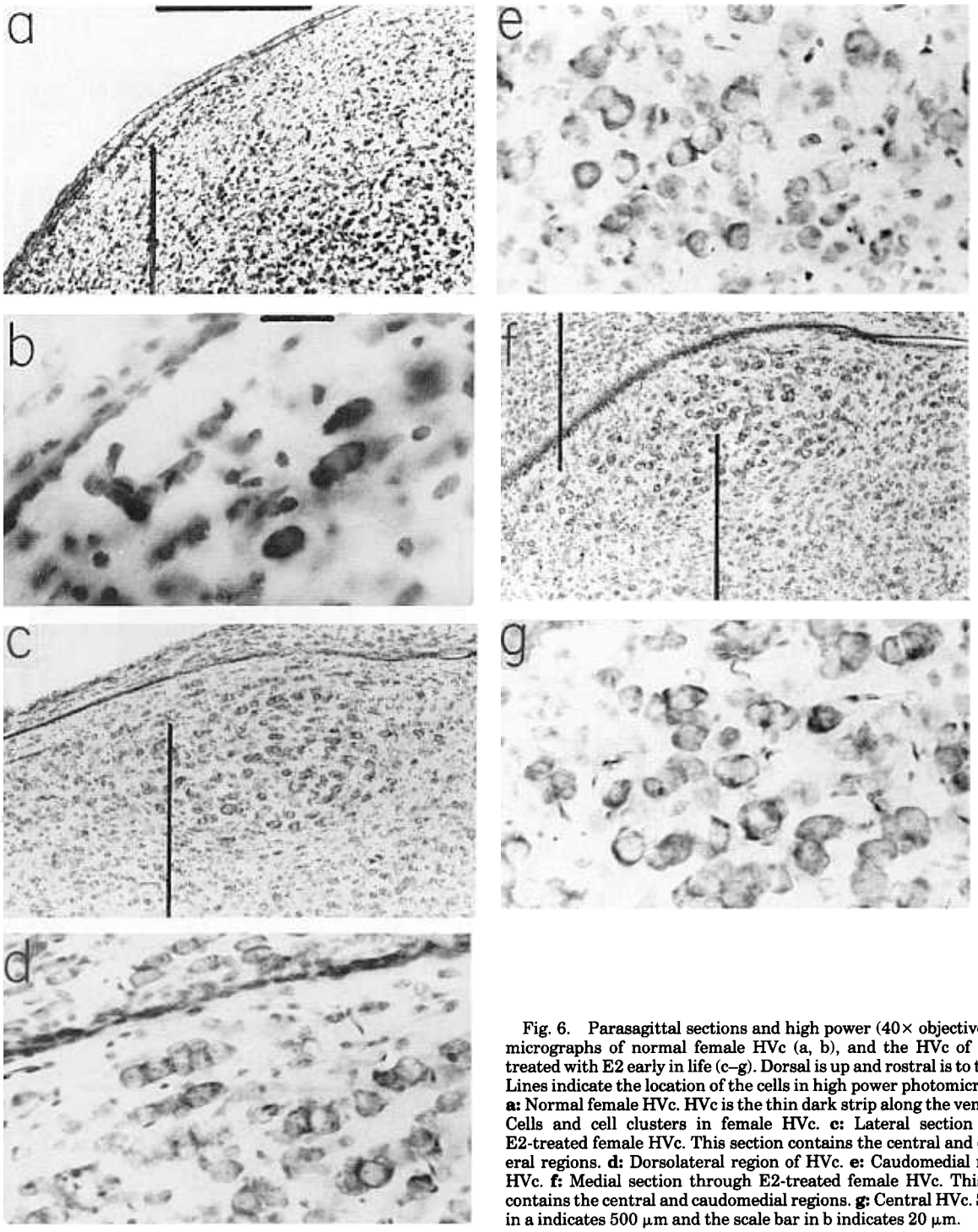

Fig. 6. Parasagittal sections and high power (40× objective) photomicrographs of normal female HVc (a, b), and the HVc of a female treated with E2 early in life (c–g). Dorsal is up and rostral is to the right. Lines indicate the location of the cells in high power photomicrographs. **a:** Normal female HVc. HVc is the thin dark strip along the ventricle. **b:** Cells and cell clusters in female HVc. **c:** Lateral section through E2-treated female HVc. This section contains the central and dorsolateral regions. **d:** Dorsolateral region of HVc. **e:** Caudomedial region of HVc. **f:** Medial section through E2-treated female HVc. This section contains the central and caudomedial regions. **g:** Central HVc. Scale bar in a indicates 500 μm and the scale bar in b indicates 20 μm.

In males, injections restricted to HVc anterogradely labeled axons which terminated in area X. Injections which included HVcand the adjacent neostriatum labeled even greater numbers of axons (Fig. 11). Most axons exited HVc rostrally or rostromedially, traveling along the medial edge of DVR either in the neostriatum or in the hyperstriatum (Fig. 11). At the level of area X these axons abruptly turned laterally and traveled into area X (Fig. 11b). This pathway is similar to one that was previously described for the zebra finch (Bottjer et al., '89). Other axons entered LH and traveled through LH to a region dorsal to area X. These axons then turned ventrally, crossing the neostriatum, and entered area X dorsally (Fig. 11a,c). Some of these axons passed through lMAN in transition to area X (Fig. 11a,c). This pathway is similar to one that was described for the canary (Nottebohm et al., '76). Other axons exited HVc ventrally and passed through the field L complex. Some of the axons continued through the neostriatum rostrally and

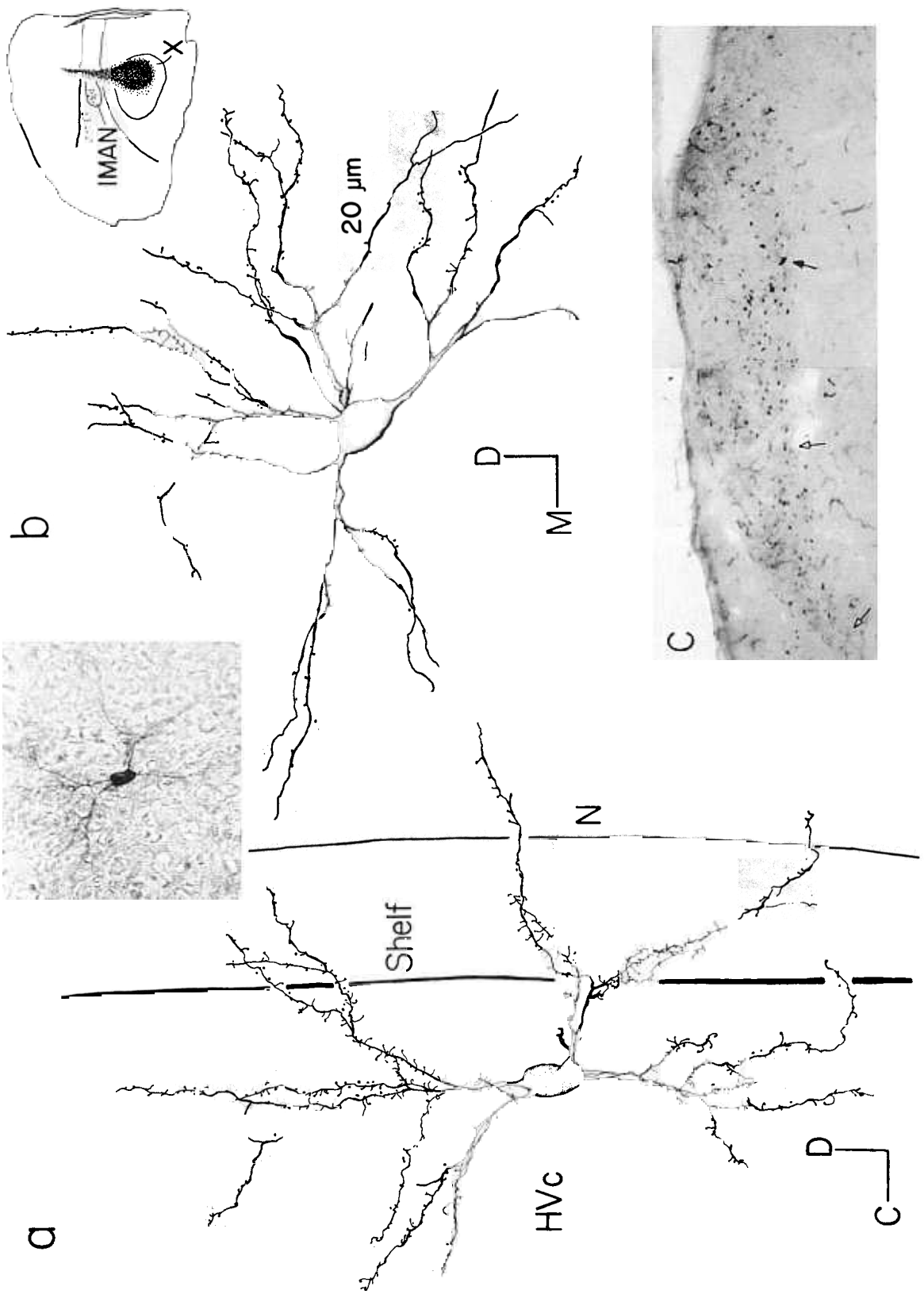

Fig. 7. Morphology and distribution of HVc cells that presumably project into area X. **a:** Case b10a. A well-filled TD_2 cell with its dendrites extending into the shelf and adjacent neostriatum. This cell was labeled by an injection into HV (injection site shown in Figure 22), and is presumed to project to area X. Similar cells were seen in HVc after injections into area X. The photomicrograph shows this neuron. **b:** Case y101b. TD_1 cell labeled by an injection into area X and surrounding tissue. Filled arrow in c indicates location of this cell. **Inset** shows the injection site. **c:** Photomontage of a single section through HVc showing retrogradely labeled cells from an injection into area X and surrounding tissue. Open arrows indicate the approximate medial and lateral borders of the caudomedial region. Central region is to the right of the caudomedial region. Note that labeled cells extend throughout the caudomedial region. Filled arrow indicates the cell drawn in b. Photomontage: 10× objective; magnification = 60 diameters.

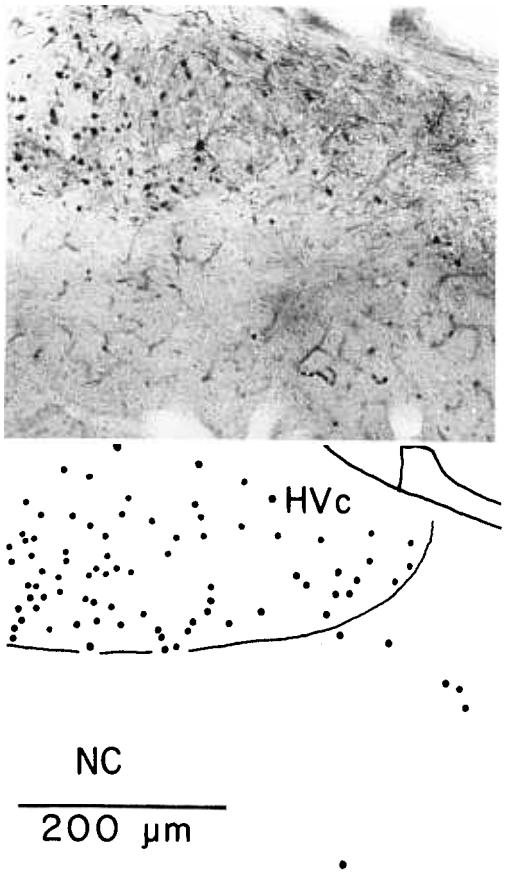

Fig. 8. Retrogradely labeled cells outside of HVc from an injection into area X and surrounding tissue. Case yl01b. Injection site shown in Figure 7b. Dorsal is up and medial is left. **Top:** Low power (10× objective) photomicrograph of a lateral portion of HVc and surrounding neostriatum. **Bottom:** Tracing of this photomicrograph indicating locations of labeled cells and boundaries of HVc.

entered area X, whereas others traveled in LMD. Lastly, some axons traveled through the paleostriatum in route to area X. These pathways, which have not been described previously, were observed in cases with injections restricted to HVc (Fig. 11a) as well as in larger injections (Fig. 11b,c).

Axons entered area X from its caudal, dorsal, and medial edges. The density of axons increased near the borders of area X, especially at the dorsal border between area X and LMD. Some axon fragments dorsal to area X extended rostrally, sometimes beyond the rostral border of area X. Axon fragments adjacent to area X, which were generally shorter than axon fragments in area X, branched occasionally, and were usually curved or bent. There were no apparent differences in the pattern of axons outside of area X between injections that were restricted to HVc and those which extended beyond the borders of HVc, though the density of efferents was greater in cases with larger injection sites. Once in area X, axons formed broad arborizations across the nucleus. Single axons could be traced in single parasagittal or coronal sections across the entire nucleus (~ 2 × 2 mm) emitting several thin, straight branches. Single axons did not form dense arbors, though area X is densely populated by HVc efferents. No varicosities were seen on any HVc axons in area X.

Projection of HVc onto RA. Injections of fluorescent dextrans (two cases) and biotinylated dextrans (three cases) into RA of males also labeled cells in each of the three subdivisions of HVc. None of these injections were restricted to RA (Figs. 12, 13). Retrogradely labeled cells were seen in all three regions of HVc, although the density of labeled cells apparently varied between the subdivisions (Fig. 12b, 13). In all five cases, the caudomedial region had the lowest density of cells, and the dorsolateral zone had the greatest density of cells (Fig. 12b, 13a,b). A quantitative analysis of the distribution of cells throughout HVc was not performed, however.

Somata that were labeled with RA injections varied in diameter from 9 μm to 15 μm. The retrogradely labeled cells appeared to be in two classes, small and medium-sized. Some cells had small round or fusiform somata (9–12 μm diameter) with lightly spined dendrites (Fig. 12a,c). These cells correspond to the short dendrite cells of Nixdorf et al. ('89). Other cells had medium-sized fusiform somata (12–15 μm diameter) and thick, densely spined dendrites. These correspond to furry dendrite (FD) cells of Nixdorf et al. ('89) (Fig. 12a,c). Cells of both morphological classes located near the ventral border of HVc had dendrites which extended into the shelf and adjacent neostriatum (Fig. 12d). Cells of each of these two types were found in each of the three subdivisions of HVc.

The axons of RA-projecting cells converged within HVc to form bundles which traveled caudally and ventrocaudally out of HVc into DA. Axon fascicles formed both within and at the caudoventral edge of HVc. Fascicles contained tens of axons. The axons of a fascicle traveled together as a unit, parallel to the caudal edge of DVR, to the dorsocaudal edge of RA. In injections of HVc that labeled RA-projecting axons (see below), fascicles were observed separating within 100 μm of the dorsocaudal border of RA. The axons then formed dense, broad arborizations in RA. Small injections into HVc, which labeled only a few fascicles, produced dense axonal arbors throughout RA.

There appeared to be a greater density of RA projecting fibers in dorsolateral HVc than in the rest of HVc (Figs. 12b, 13a,b). This is particularly evident in parasagittal material, because the axons travel in the sagittal plane. The axons in dorsolateral HVc are not arranged in tight bundles, as is seen in the rest of HVc and as is seen caudal to HVc as the axons enter DA (Fig. 13). There were also a few cells labeled in NC caudal and ventral to HVc (Figs. 12, 13). Most of these cells are caudal to HVc in or near DA, and are often surrounded by bundles of HVc fibers (Fig. 13). The density of labeled cells in NC was considerable lower than that in HVc. These NC cells probably project to the archistriatum adjacent to RA, because injections into NC adjacent to HVc anterogradely label axons surrounding RA (see Fig. 16). RA injections also labeled cells throughout lMAN, as has been previously reported (Nottebohm et al., '82; Bottjer et al., '89). Lastly, the injections into RA and the adjacent archistriatum also labeled cells throughout the archistriatum and in L1 and L3 of the field L complex (Fig. 12, inset). Well-filled cells in field L were either type 1 or type 2 (see Fortune and Margoliash, '92a). Most of the retrogradely labeled cells were in L3, though there were labeled cells throughout both L1 and L3.

Intrinsic projections of HVc. Injections involving HVc (N = 10, including fluorescent and biotinylated dextrans; see below) labeled cells throughout HVc (Fig. 14). Any injection site which impinged on any of the three regions of HVc labeled cells in all three regions of HVc. We could not distinguish whether cells were labeled via their intrinsic or

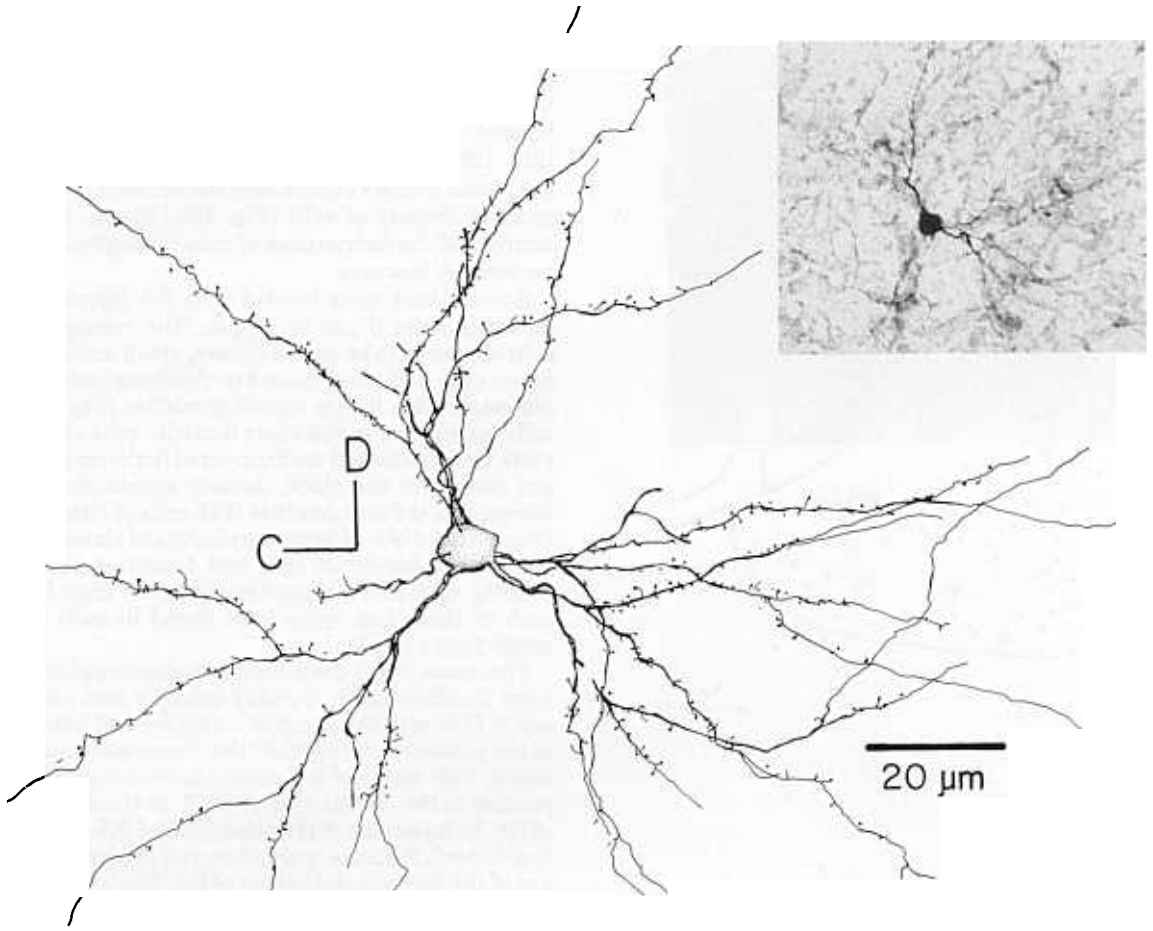

Fig. 9. A new class of cell that presumably projects to area X. Case b09a. The retrogradely labeled cell is characterized by a small somata, a large dendritic arborization, and thin dendrites with relatively few spines. The injection site is shown in Figure 22.

extrinsic projections; however, HVc neurons have extensive intrinsic arborizations (see Katz and Gurney, '81). The distribution of labeled cells in HVc was different in each case. In one case (see Fig. 14), there was dense labeling in the caudomedial region and less in central HVc. In other cases, few cells were labeled in the caudomedial region and labeling was dense in central and dorsolateral HVc (not shown). Nevertheless, we were unable to determine any consistent topographical pattern across cases, even though we had a relatively large number of cases. The differences in the pattern of labeling throughout HVc between cases may be due to real, idiosyncratic differences in connectivity, or may be due to patchiness resulting from variations in the quality of staining (see Discussion).

Afferents of HVc

These data are presented in three parts. First, we describe the afferents of HVc based on restricted injections into HVc. Most significantly, we show evidence for a projection to HVc from neurons in the field L complex that are broadly distributed in L1 and L3. Next, we describe the results of larger HVc injections that also encroached on NC. These data, in combination with data from control injections that did not include HVc, demonstrate that NC adjacent to HVc has a pattern of afferents and efferents similar to that of HVc. The control injections we describe in the last part include anterograde data that serve to confirm the retrograde results. Additionally, the control injections demonstrate a projection from a region surrounding Uva to HV.

Patterns of retrograde labeling from injections restricted to HVc

Four injection sites were restricted to HVc; these injection sites did not encroach upon the shelf or adjacent neostriatum. Injection sites with biotinylated dextrans were considered to be restricted to HVc if they met two criteria: first, the area of cellular damage and extracellular detritus caused by the injection was contained within the cytoarchitectonically determined boundaries of HVc (Fig. 15a–c). For fluorescent cases the borders of HVc were more difficult to determine, but in this material, which was not counterstained, the shelf was visualized with Nomarski optics. Second, anterograde labeling in the archistriatum was restricted to RA (Fig. 15d). In contrast, all five injection

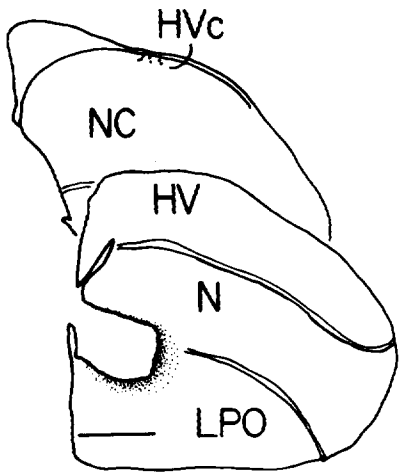

Fig. 10. Retrograde labeling in female HVc from an injection of retrograde tracer into LPO and the frontal neostriatum. Case f02a. Dorsal is up and medial is left. All of the retrogradely labeled cells (N = 7) in HVc were in the one section shown here. There were other cells labeled in the caudal neostriatum ventral to HVc, which are not present in this section. Scale bar indicates 1 mm.

sites which extended into the neostriatum adjacent to HVc (Fig. 15e) labeled arbors adjacent to and surrounding RA (Fig. 15f). Two injection sites were located in DA, just caudal or caudolateral to HVc but avoiding HVc itself. These injections densely labeled axons surrounding RA, and labeled axons within RA but at a lower density (Fig. 16). Because these injections must have interrupted HVc axons projecting to RA (e.g., see Fig. 13), the high density of fibers surrounding RA probably did not result from labeling fibers-of-passage.

Two restricted injections (b06a, b13a) involved only central HVc and the dorsolateral zone that contains oriented cells and cell clusters. The third injection (f01a) involved all three regions of HVc. The fourth injection (b03b) was situated primarily in the caudomedial region, though it also included the central region. In a fifth case (b16b), the injection site was situated in the caudomedial region of HVc, and did not invade the central region. Because the ventral border of the caudomedial region is not distinct, and because this case produced almost no anterograde staining, we were unable to confirm that this injection site did not invade the adjacent neostriatum. All five of these injections, however, produced the same pattern of retrograde labeling. These injections retrogradely labeled cells in L1 and L3 of the field L complex, throughout HVc, in the thalamic nucleus Uva and in the nuclei mMAN and NIf. A few cells were labeled in L2a, and possibly some cells in L2b at its border with L1.

Distribution of cells in the field L complex. Injections of biotinylated dextrans restricted to HVc labeled cells in L1 and L3 of the field L complex (Fig. 17a). The rostral extent of labeling in L1 varied between birds, but no cells were seen more than 1.5 mm rostral of the intersection of L2a and LMD in parasagittal material and most cells in L1 were within 1 mm of this intersection. (The rostral border of L1 is not distinct; see Fortune and Margoliash, '92a.) Some of the retrogradely labeled cells in dorsal-most L1 may have been in L2b, as the border between L1 and L2b is not distinct. L3, which has distinct borders, also contained labeled cells (Fig. 17a). More cells were labeled in L1 than in L3 in all cases.

There was no apparent topography of labeled cells within L1 or L3, with labeled cells distributed throughout L1 and L3. Retrograde labeling in the field L complex was relatively sparse, however, especially in cases of injections of biotinylated dextrans that were restricted to HVc, where only tens of cells were retrogradely labeled in the field L complex (Fig. 17a). Furthermore, there was variation in the quality of staining between sections in some biotinylated dextran cases. These two factors may have masked any topography in the biotinylated cases. Fluorescent material exhibited many more labeled cells, and much more uniform staining across the tissue, however. For example, a restricted injection of fluorescent tracer (case f01b) had uniform staining across all sections. In this case, hundreds of cells were labeled in the field L complex, and the density of labeled cells in L1 and L3 appeared to be similar (Fig. 18). The distribution of cells in the field L complex in fluorescent material was apparently the same as in the biotinylated material, though cell types (see below) were not identifiable in the fluorescent material.

Individual axons of some labeled field L cells could be traced for several hundred microns. Because individual axons could not be traced all the way to HVc, the pathway of axons was inferred from the pattern of labeled axonal fragments. Axons from L1 cells traveled dorsally or dorsocaudally through L1. Some of these axons remained below LH and others entered LH. These axons then traveled caudally across the dorsocaudal neostriatum, crossing through L2b or dorsal to L2b, and entered either HVc or the shelf at their rostral borders. Axons from L3 cells traveled dorsally through L and L2b of the field L complex before turning caudally along the ventricle. These axons entered either the shelf or HVc from their rostral borders. This analysis is confounded by labeled fragments of fibers from NIf and Uva axons, which were not distinguished from axons of cells in the field L complex. Nevertheless, these pathways are consistent with the projection of axons of Golgi-stained field L neurons in the European starling (*Sturnus vulgaris*) (Saini and Leppelsack, '81).

Morphology of cells labeled in the field L complex. 'Most of the cells labeled in L1 and L3 were not filled well enough to be classified into morphological types because the differences between cell types in the field L complex relies heavily on dendritic morphology. Those cells that were morphologically identifiable were either types 1 or 2 as defined in Golgi material (Fortune and Margoliash, '92a). Type 1 cells have large ($\sim$12 μm diameter), triangular somata and thick (2–3 μm), long and densely spined dendrites (Fig. 19a). Type 2 cells have medium-sized (8–10 μm diameter) somata with sparsely spined dendrites (Fig. 19b). Occasionally some type 3 oriented neurons were labeled in L2a (not shown). Type 3 oriented cells have medium-sized (8–10 μm diameter), ovoid somata with bipolar dendrites that are sparsely covered with spines. Type 4 neurons, the smallest type of neurons seen in Golgi preparations of the field L complex, may also have been labeled by injections into HVc, but we were unable to determine if the apparent type 4 neurons were simply poorly filled examples of the larger types of neurons.

Morphology of cells labeled in NIf. HVc injections labeled cells throughout NIf. The labeling in NIf was dense, and generally, NIf cells were better filled than cells in other nuclei. The projection of NIf cells onto HVc does not appear

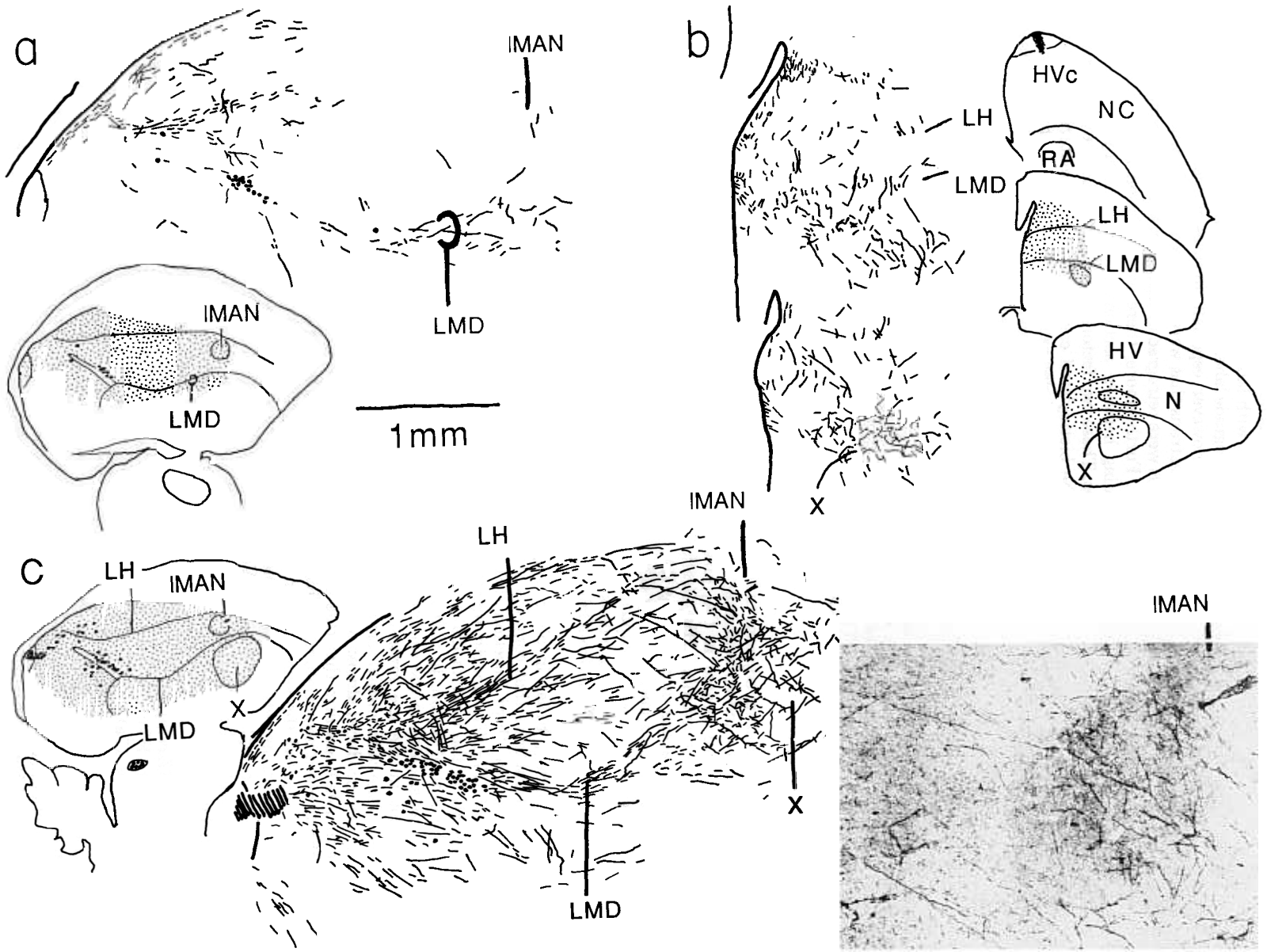

...s from HVc to area X. This figure shows
correspond to restricted (a), almost restricted (b), and
njections of HVc. The stippled areas on the overview correspond to the areas shown at higher power. The labels on the higher power views are in the same relative b13a. Dorsal is up and rostral is to the right. The in Figure 1a. **b:** Case b04b. Dors and lateral is to the right. **c:** Case b10b. Dorsal is up and rostral is to the right. The thick line near lMAN in the two drawings corresponds to a piece of detritus seen in the photomicrograph at the right. The lines pointing to lMAN are just dorsal and rostral to the nucleus, which can be seen in the photomicrograph as the oval region that is darker than the background.

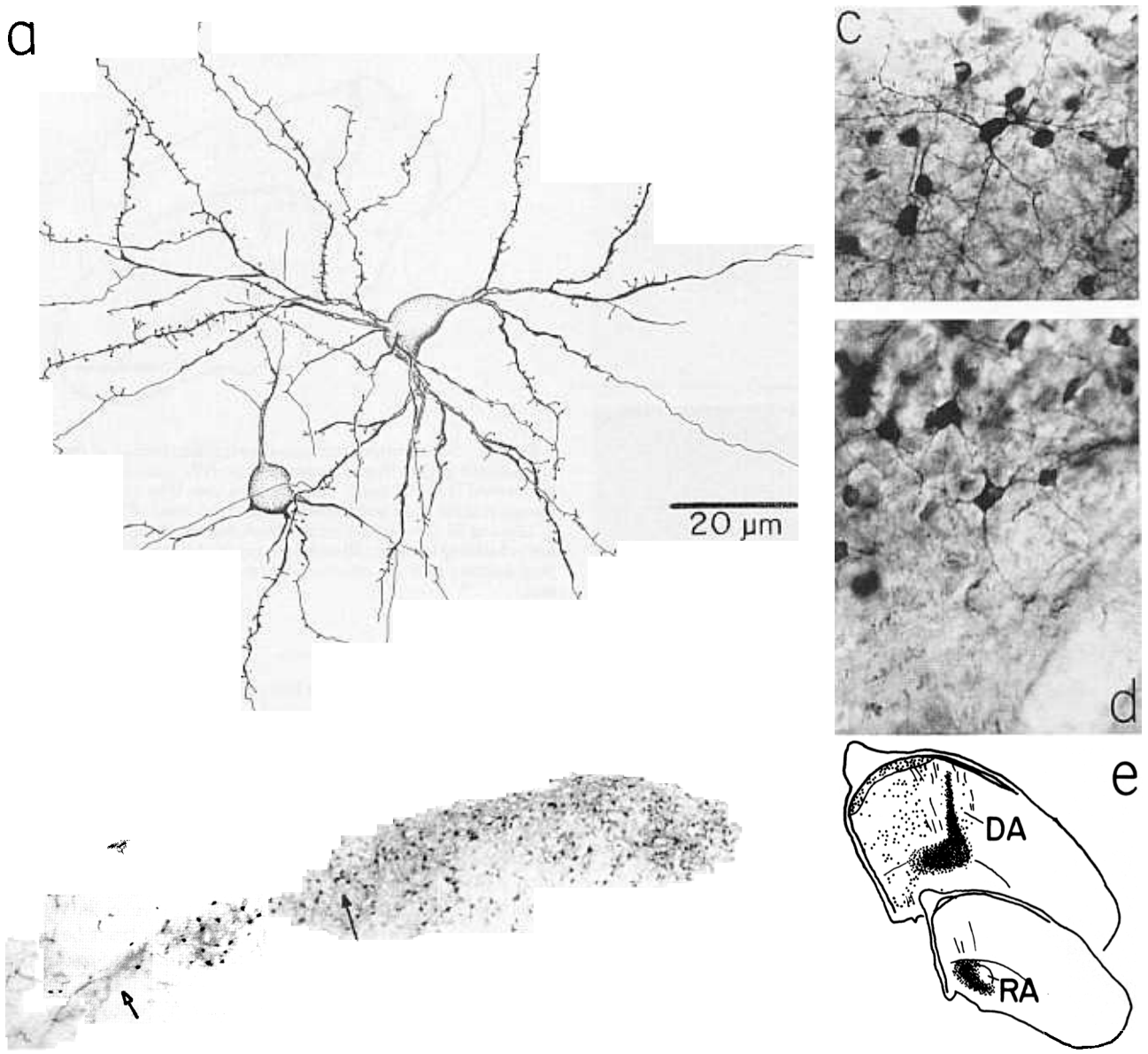

Fig. 12. Morphology and distribution of HVc cells that presumably project to RA. Case yl01a. Dorsal is up and medial is left. **a:** Retrogradely labeled FD cell (larger soma) and SD cell (smaller soma) from the injection shown in **e**. The site was centered on DA adjacent to RA, but impinged on a large area of RA. **b:** Photomontage of a single section through HVc showing retrogradely labeled cells. Open arrow indicates the medial border of the caudomedial region of HVc. The closed arrow points to the cells drawn in a and indicates the approximate lateral border of the caudomedial area. Note the greater apparent density of cells and axons along the dorsal edge of the central region (to the right of the filled arrow). Photomontage: 10× objective, magnification 60 diameters. **c:** High power (40× objective) photomicrograph of the cells shown in a. **d:** High power photomicrograph of cells along the ventrolateral border of HVc with dendrites extending into the shelf. Both FD and SD cells had dendrites extending into the shelf.

to be topographic. Small injections into HVc labeled fewer cells in NIf than did larger injections, but in all cases the labeled cells were seen throughout NIf. Most of the labeled cells in NIf had the morphological characteristics of type 5 cells as seen in Golgi material (Fortune and Margoliash, '92a), including oval or oblong somata with both thick (2–3 mm diameter) and medium (1 μm diameter) dendrites that were sparsely covered with spines (Fig. 20). On occasion, NIf cells along the rostral border of NIf labeled by HVc injections had dendrites which extended into adjacent L1 (Fig. 21). Such NIf cells had fusiform somata, not oblong as is typically the case for NIf cells. These cells may represent a separate morphological type of NIf neuron that receives input from L1 (see Discussion). Axons from cells in NIf exited NIf dorsally and traveled either within L2a or through L1. The pathway of NIf axons was inferred from the pattern of axon fragments. Axons apparently turned caudally below or in LH and traveled parallel to the ventricle above the field L complex into rostral HVc.

Morphology of cells labeled in Uva. Injections restricted to HVc also labeled cells in the dorsal thalamic nucleus Uva (Fig. 20). Neurons throughout Uva project to

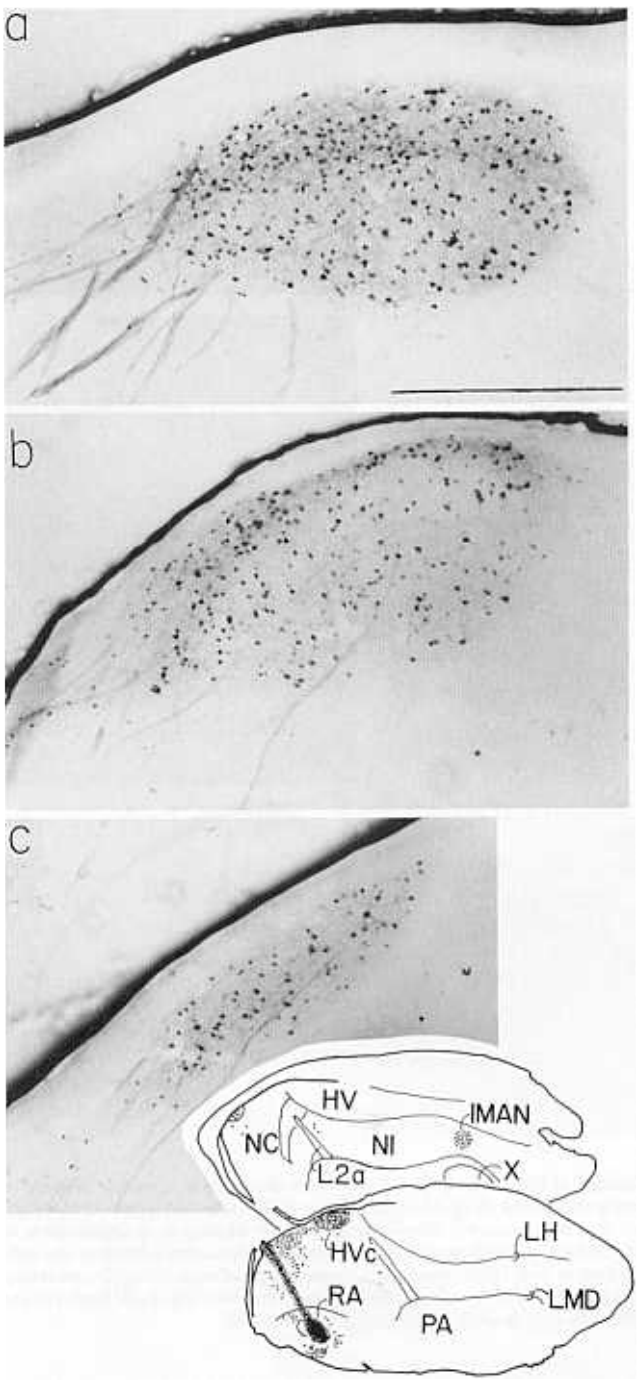

Fig. 13. Retrograde labeling in HVc from an injection of retrograde tracer into RA. Case bb14a. Dorsal is up and caudal is left. **Inset** shows the injection site into RA and the adjacent archistriatum. Photomicrographs are of parasagittal sections from lateral (a) to medial (c). **a:** Central HVc and the dorsolateral zone. **b:** Central HVc and the small celled region. **c:** Medial HVc showing central and small-celled regions. Note the greater apparent density of labeled cells and axons along the dorsal border in a and b. There were retrogradely labeled cells in L1 and L3 in sections medial to those shown in the **inset**, and there were many retrogradely labeled cells in the caudal neostriatum adjacent to HVc (**inset**). Scale bar indicates 500 mm.

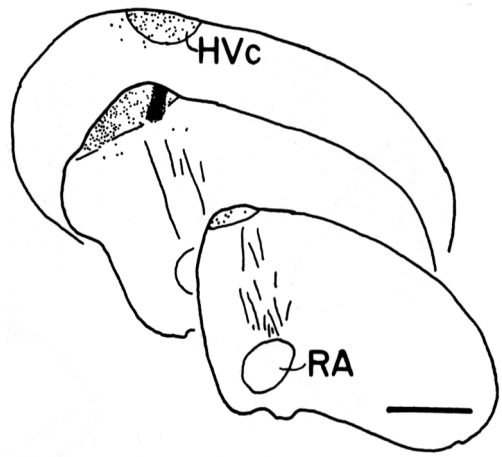

Fig. 14. Serial coronal sections showing distribution of retrogradely labeled cells in HVc from an injection into HVc. Case b11a. Dorsal is up and lateral is to the right. This injection into HVc encroaches slightly upon the shelf. Cells were labeled in all three areas of HVc. The density of labeling in the regions varied from case to case; this case showed heavy labeling in the small-celled region (middle section), and relatively little labeling near the injection site (see Results). Scale bar indicates 1 mm.

HVc. In those cases where few cells were labeled in Uva (see Fig. 22c) the cells were spread across the nucleus. Cells at the periphery of Uva, especially along the dorsal edge, were often flattened and oriented along the edge of the nucleus. Cells were either large, with round somata (13–17 μm diameter) and thick (~2 μm diameter) stumpy dendrites or small with fusiform somata (8–10 μm diameter) with thin (~1 μm diameter) elongate dendrites (Fig. 20). Uva dendrites appeared lumpy, having fusiform varicosities distributed along their lengths. Axons from Uva cells traveled rostrally and rostromedially in a thin fiber tract below the dorsal thalamic group. Most axons turned dorsally and entered the lateral forebrain bundle between Ov and DLM. Some axons traveled around the ventral border of Ov and entered the lateral forebrain bundle at the rostral edge of Ov. Axons followed the lateral forebrain bundle, turning medially and then dorsally, into DVR. In DVR the axons passed through the caudal pole of the paleostriatum primitivum (PP) and entered the field L complex. Uva axons in the field L complex were not distinguishable from anterogradely labeled axons en route to area X and retrogradely labeled axons from cells in the field L complex and NIf. As a result, we were unable to determine the exact pathway of these axons through the field L complex and into HVc.

Morphology of cells labeled in mMAN. Injections into HVc also labeled cells in mMAN. This nucleus is not cytoarchitectonically distinct in the zebra finch (see Bottjer et al., '89). mMAN cells were seen along LMD (Fig. 20) medial to the cytoarchitectonically distinct lMAN. The labeled cells in mMAN were stellate with small and medium-sized somata (8–13 μm diameter) (Fig. 20). There are probably more than one morphological class of cells, based on the distribution of soma sizes. mMAN dendrites are spiny. We were unable to determine the paths of mMAN axons, in part due to the large number of HVc efferents which travel adjacent to mMAN and enter area X.

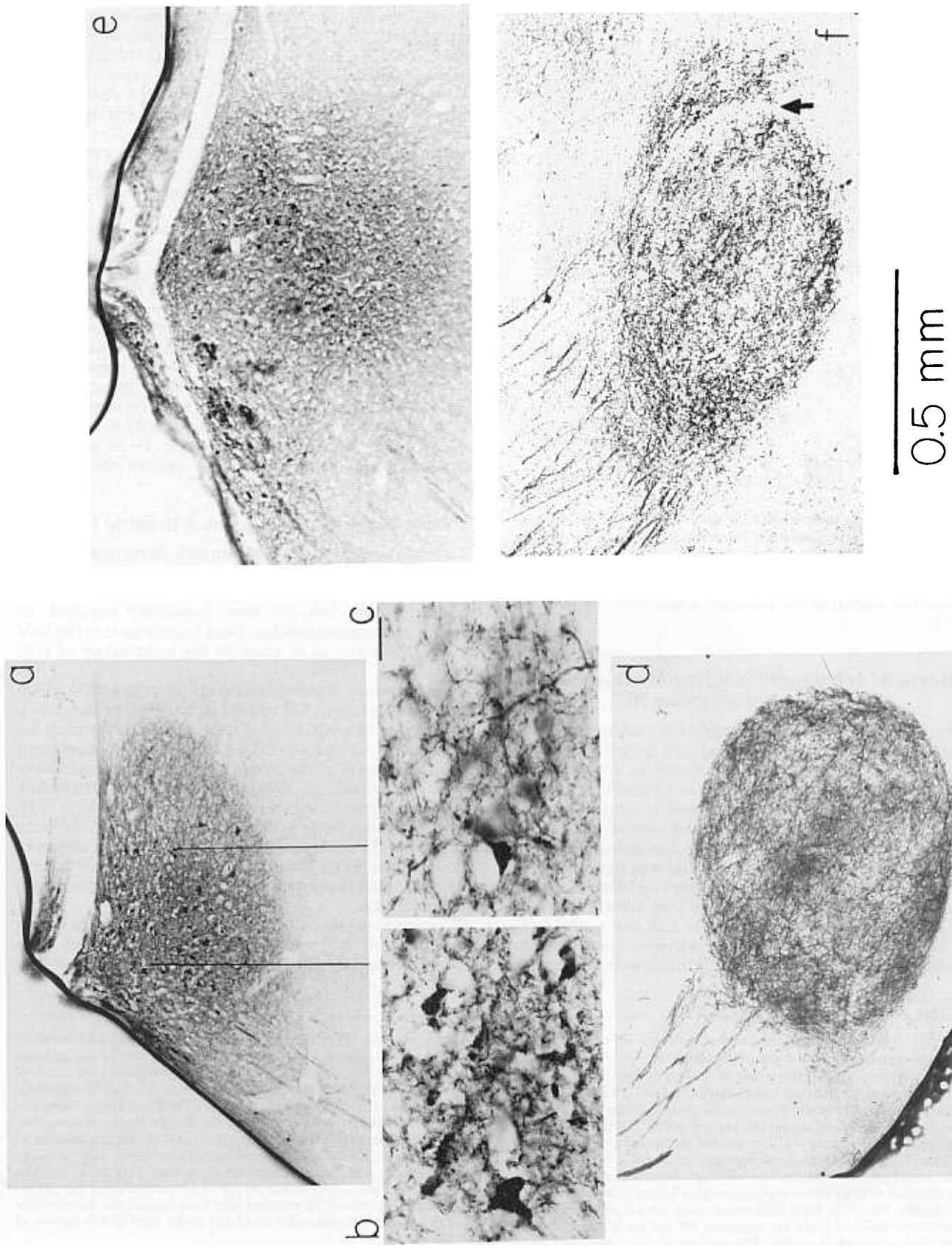

Figure 15

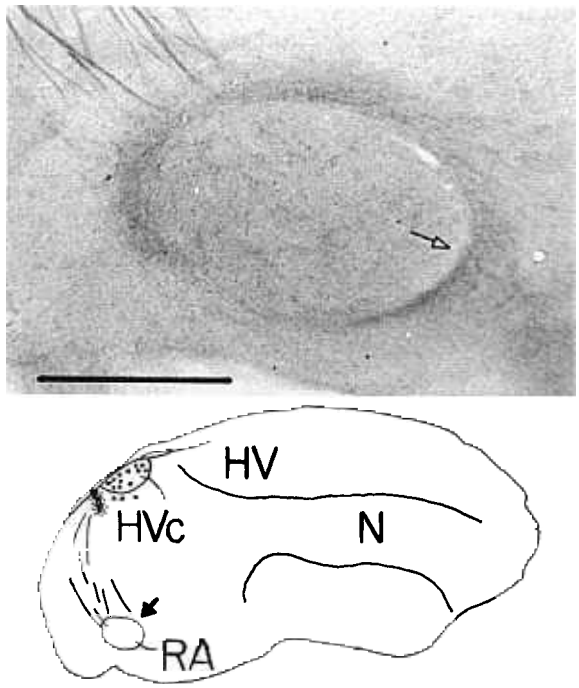

Fig. 16. Anterogradely labeled axons in and around RA from an injection caudal to HVc. Case b15a. Dorsal is up and caudal is left. **Top:** Dense anterograde labeling around RA and light labeling within RA. Arrow indicates a thin crescent along rostral RA that does not contain labeled fibers. **Bottom:** Injection sites and retrograde labeling. Arrow indicates the location of the photomicrograph. Scale bar indicates 200 μm.

Patterns of retrograde labeling from injections into HVc and adjacent NC

Five injections of HVc also invaded the shelf and adjacent neostriatum. These injections produced, in addition to the retrograde pattern of labeling produced by injections restricted to HVc, retrograde labeling in HVand NC. Labeled neurons in HV were dorsal to the field L complex. In one case, labeled cells in HV were located rostrally in medial sections and moved caudally in more lateral sections (Fig. 17b). A topographic pattern of labeling was not evident in the other cases. Labeled cells in HV were stellate, spiny, and had medium-sized and large somata (not shown). Labeled cells in NC were found both dorsal to L2b and caudal to L. Unlike labeling in L1, L3, and HV, where cells appeared to be relatively evenly distributed, cells in NC were labeled in a patchy distribution (Fig. 17b). These larger injections of HVc also labeled greater numbers of cells in the field L complex, NIf, and Uva than did injections that were restricted to HVc. We did not resolve whether the increased number of labeled cells resulted from the larger size of the injections or from involvement of afferents that terminate ventral to HVc. Labeled cells in L1 were found medial to those of L3 in parasagittal sections (Fig. 17b). This obtained because L1 extends medially to L3 (Fortune and Margoliash, '92a). In coronal sections where both L1 and L3 were present, there was no apparent difference in the distribution of cells within these subdivisions.

Injections into HVc and the adjacent neostriatum anterogradely labeled axons in and adjacent to area X and RA (Fig. 15e,f; also see Fig. 11). We saw no evidence for anterograde labeling of a nucleus Avalanche in HV as has been tentatively identified in the canary (Nottebohm et al., '82). The pattern of projections onto area X and within RA was not different from that produced by injections restricted to HVc. The pattern of anterogradely labeled axons around RA varied greatly between injection sites. In some cases there was extensive labeling rostral and rostromedially to RA. In others, axons formed a dense plexus dorsal to RA (Fig. 15f). However, in all cases, a thin (~50 μm thick) crescent along the rostral edge of RA was not labeled (Figs. 15f, 16).

Injection sites that did not include HVc

We made control injections into structures surrounding HVc, including HV, NC, and the field L complex. As well as control data, these injections also provided information on connectivity that has not been previously reported. In addition, anterograde labeling from injections into the field L complex allowed us to examine the morphology of HVc afferents.

HV injections. Two birds with injections into HV, which also encroached upon LH and NI just rostral to the field L complex, retrogradely labeled cells and anterogradely labeled axons in L1 and L3 of the field L complex, in adjacent HV, in the caudal neostriatum ventral to HVc, and retrogradely labeled cells in HVc and in a region surrounding dorsal, dorsocaudal, and dorsorostral edges of Uva (Fig. 22a,b). Two injections of fluorescent dextrans that were restricted to HV confirmed the pattern of labeling shown in Figure 22, including labeling cells adjacent to Uva (not shown). A small number of retrogradely labeled cells were also seen in L2a.

HV injections labeled at least two types of cells in the region adjacent to Uva (Fig. 22a). Some cells had large oblong somata (12–15 μm diameter) with long, slender

Fig. 15. Injections of biotinylated dextrans into HVc. Dorsal is up and rostral is to the right. a–d are from case b13a, e and f are from case b10b. **a:** Low power photomicrograph of the section through the largest extent of an injection site that was restricted to HVc. The shape of HVc was distorted dorsally by the injection electrode. Streaks at the bottom left corner are bundles of axons that project to RA. The thick black line along the dorsal border of HVc is a bubble on the slide. Lines indicate locations of high-power photomicrographs in b and c. **b:** High power photomicrograph from within the injection site. Notice the granular black detritus. **c:** High power photomicrograph from just outside of the injection site. There are filled cells and densely labeled neuropil, but no extracellular detritus. Scale bar indicates 20 μm for b and c. **d:** Low power photomicrograph of RA. The streaks in the upper left hand corner are bundles of axons from HVc. RA is densely filled with axonal arborizations from HVc. There are only a few arborizations outside of RA at its caudal edge. **e:** Low power photomicrograph of the greatest extent of an injection site into HVc, the shelf, and adjacent neostriatum ventral to HVc. Bundles of axons projections to RA and surrounding regions can be seen in the lower left corner. The black streak along the parahippocampus is a bubble on the slide. **f:** Low power photomicrograph of RA. The streaks in the upper left hand corner are bundles of axons from HVc. RA and adjacent archistriatum dorsal and rostral to RA are densely filled with axonal arborizations from HVc and the adjacent neostriatum. The arrow points to a crescent along the rostral and rostrodorsal edge of RA with few labeled arborizations. Label to the left of this crescent is within RA and label to the right of it is outside of RA.

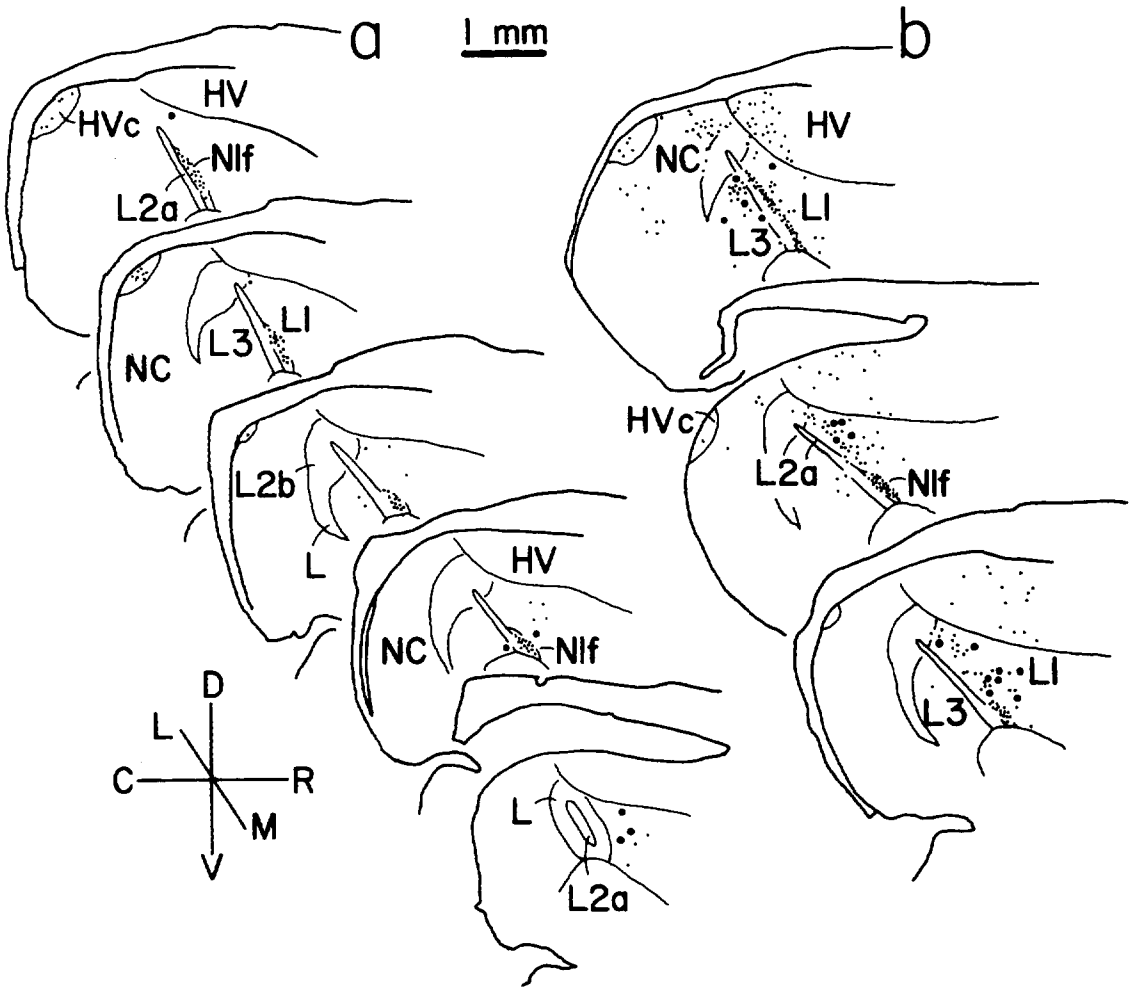

Fig. 17. Serial parasagittal sections showing pattern of retrograde labeling from injections into HVc. Large dots indicate the positions of retrogradely filled type 1 cells in the field L complex, and small dots indicate the positions of all other cell classes (see Fortune and Margoliash, '92a). There are no type 1 cells in NIf; the large dots in NIf result from clusters of small dots. **a:** Case b13a. The injection site is shown in Figure 15a. There were many cells labeled in NIf and throughout HVc. A few cells were labeled in L1 and L3. Labeled cells in mMAN and Uva are not shown. **b:** Case b10b. The injection site is shown in Figure 15e. Cells were labeled in L1, L3, HV, NC, and HVc. Labeled cells in mMAN and Uva are not shown.

dendrites that extended more than 200 μm. The dendrites of these cells often ran parallel to the border of Uva, and were not seen entering Uva. There were also stellate cells with medium-sized somata (10–13 μm diameter). The dendrites of these cells did not extend more than 100 μm from the soma, and the arborizations were roughly spherical. Neither of these cell types had spines on their dendrites, though the dendrites did have thickenings on them (Fig. 22a). Uva cells are also free of spines (Fig. 20). The morphology of the cells surrounding Uva are nevertheless distinct from Uva cells, which have round somata and stumpy dendrites (Fig. 20). Some HVc neurons were labeled by these injections. These neurons presumably projected to area X, their axons traveling through HV in route to area X (see Fig. 11).

NC injections. Two injection sites into the caudal neostriatum just rostral to HVc retrogradely labeled cells in L1, L3, NIf, HV, HVc, Uva, and in and around Ov (not shown). These injections anterogradely labeled axons in area X. The retrogradely labeled cells in both of these cases were not filled well enough to be identified. Two injection sites caudal to HVc, both of which impinged upon DA, retrogradely labeled cells in HVc and the adjacent neostriatum (Fig. 16). Some anterogradely labeled axons entered RA, whereas most remained outside of RA (Fig. 16). Axons completely surrounded RA; though, as in other injections into the neostriatum adjacent to HVc (see above), there were no axons labeled in a thin crescent along the rostral border of RA (Figs. 15f, 16). In all four cases, we interpret the labeling of HVc cells as resulting from interruption of axons projecting to area X or to RA (see Discussion).

Injections into the field L complex. We placed two large injections into the center of the field L complex. Both injection sites included L1, L2a, L3, and NIf. One of the two injections crossed LMD and entered the paleostriatum augmentatum (PA). In addition, we placed one injection in rostral L1 and another injection that primarily involved L3. All four injections retrogradely labeled cells in HV, NC, A, HVc, L1, L2, L3, and Ov (Fig. 23c). The two large injection sites in the center of the field L complex also labeled some

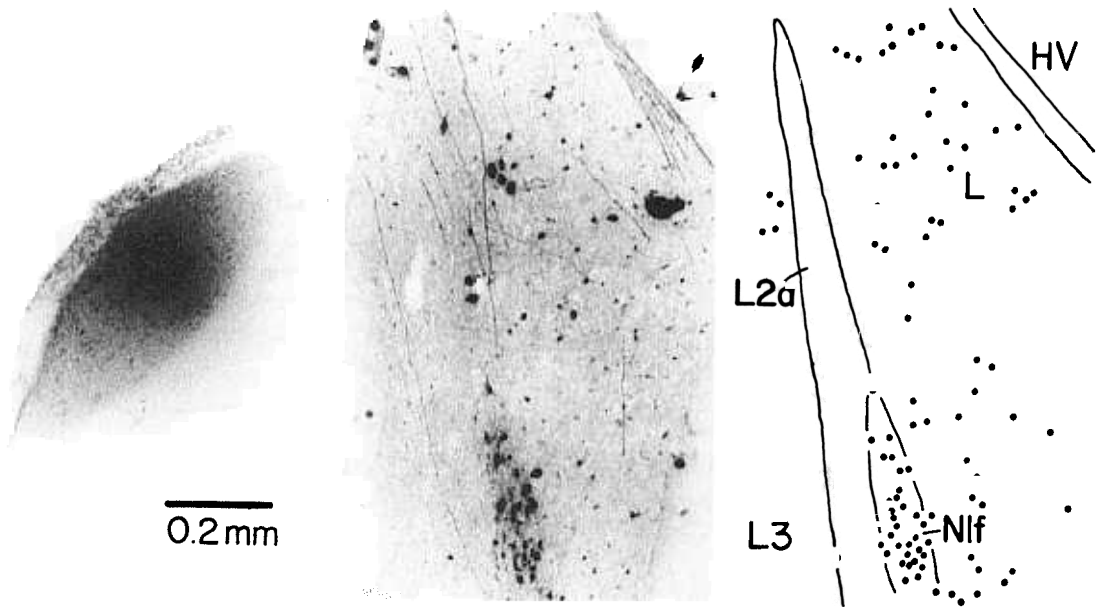

Fig. 18. Injection of fluorescent dextrans into HVc (case f01b). Dorsal is up and caudal is left. The photomicrographs are negatives of the section. **Left:** Photomicrograph of the injection site, restricted to HVc. The ventral border of HVc was determined and the extent of the injection site confirmed using Nomarski optics. **Middle:** Photomicrograph of the field L complex, NIf, and HV. The streaks are anterogradely and retrogradely labeled axons, the large dark spots are artifacts, and the light, small dots are retrogradely filled cells. **Right:** Drawing of the adjacent photomicrograph showing the positions of filled cells (dots) and the borders of the structures.

cells in PP and PA (not shown) as well as in Uva (Nottebohm et al., '82). One of these two large injection sites also labeled cells in lMAN (not shown). There were differences in the pattern of labeling within some of the structures that were labeled in all four cases, particularly within the field L complex itself and in and around Ov. Thus, we provide preliminary evidence in the zebra finch for reciprocal connections between field L and HV, connections between field L subdivisions, and differential projections of Ov and surrounding structures onto the field L complex (see Discussion). A detailed description of these pathways, however, is beyond the scope of this paper (see Karten, '67, '68; Bonke et al., '79a; Kelley and Nottebohm, '79; Brauth et al., '87; Bell et al., '89; Wild et al., '90; Fortune and Margoliash, '91, '92a; Durand et al., '92).

The injections into the field L complex also anterogradely labeled axons within HVc and ventral to caudolateral HVc (Fig. 23a,b). The labeling in three of these cases was sparse, having only a few axons in and around HVc. One case, a large injection into the center of the field L complex, densely labeled axons in and around HVc. Most of the axons in the shelf and adjacent neostriatum ran parallel to the shelf in the sagittal plane, though some axons ventral and caudolateral to HVc formed a dense, fusiform plexus that was approximately 300 μm in diameter. Within HVc, few axons were labeled dorsally. These axons were medium to thick and ran parallel to the ventricle in the sagittal plane without branching. Ventrally there were dense axonal arborizations. The majority of these fragments were thin and branched often. Some of these axons had small varicosities on them. There were also thick, rough or varicose axons which branched infrequently to form arborizations that covered several hundreds of microns (Fig. 23a). These thick varicose axons were not seen along the ventral border of HVc. Axons in ventral HVc were thin and branched often. Nomarski microscopy showed that these axons surround and probably contact somata. Axons in the shelf and along the ventral border of HVc were thin or medium-thickness and ran parallel to the shelf itself. Axons ventral to HVc formed a dense plexus with very many thin (1 μm diameter) axons that branch frequently.

DISCUSSION

We have described the cytoarchitectonic organization, connectivity, and morphology of afferent and efferent cells of HVc. The cytoarchitectonic analysis demonstrates HVc has three subdivisions, and helps to resolve issues regarding the definition of HVc and the shelf ventral to HVc. The tracer studies demonstrate that all subdivisions of HVc receive multiple, parallel non-topographic inputs and send divergent outputs. Additionally, one or more areas ventral to HVc have a similar pattern of connectivity as HVc. We describe several new cell types, including a new class of X-projecting HVc neuron and new classes of NIf and Uva neurons that project to HVc. Many of these inputs to HVc may carry auditory information. These data are interpreted in relation to the functional properties of HVc and in relation to the origins of the song system.

Definition of HVc

The data demonstrate that HVc in male zebra finches has three subdivisions whose relation to each other and to the shelf are complex, and that some of the borders of HVc, especially the ventral caudomedial border, are not distinct. Whereas the central region is commonly recognized as HVc, the dorsolateral region of oriented cells has also apparently been included, if not recognized, as part of HVc in most studies. There has also been some question whether the

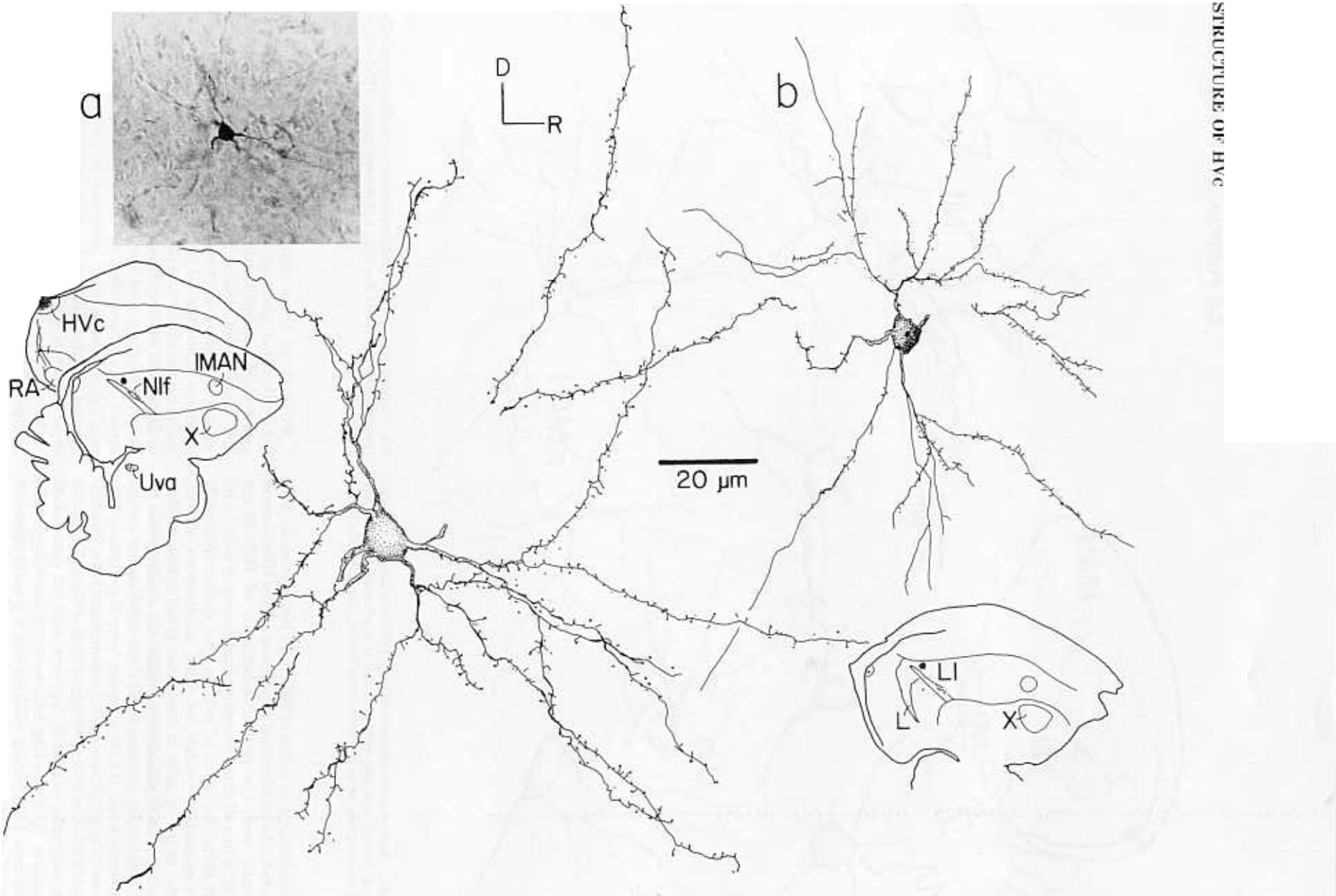

Fig. 19. Camera lucida drawings of retrogradely labeled cells from an injection restricted to HVc. Case b13a (see Figure 14a). **a:** Type 1 cell. **Insets** show the injection site, the location of the cell in L1 (large dot), and a photomicrograph of the cell. **b:** Type 2 cell. **Inset** shows the location of the cell in L1 (large dot).

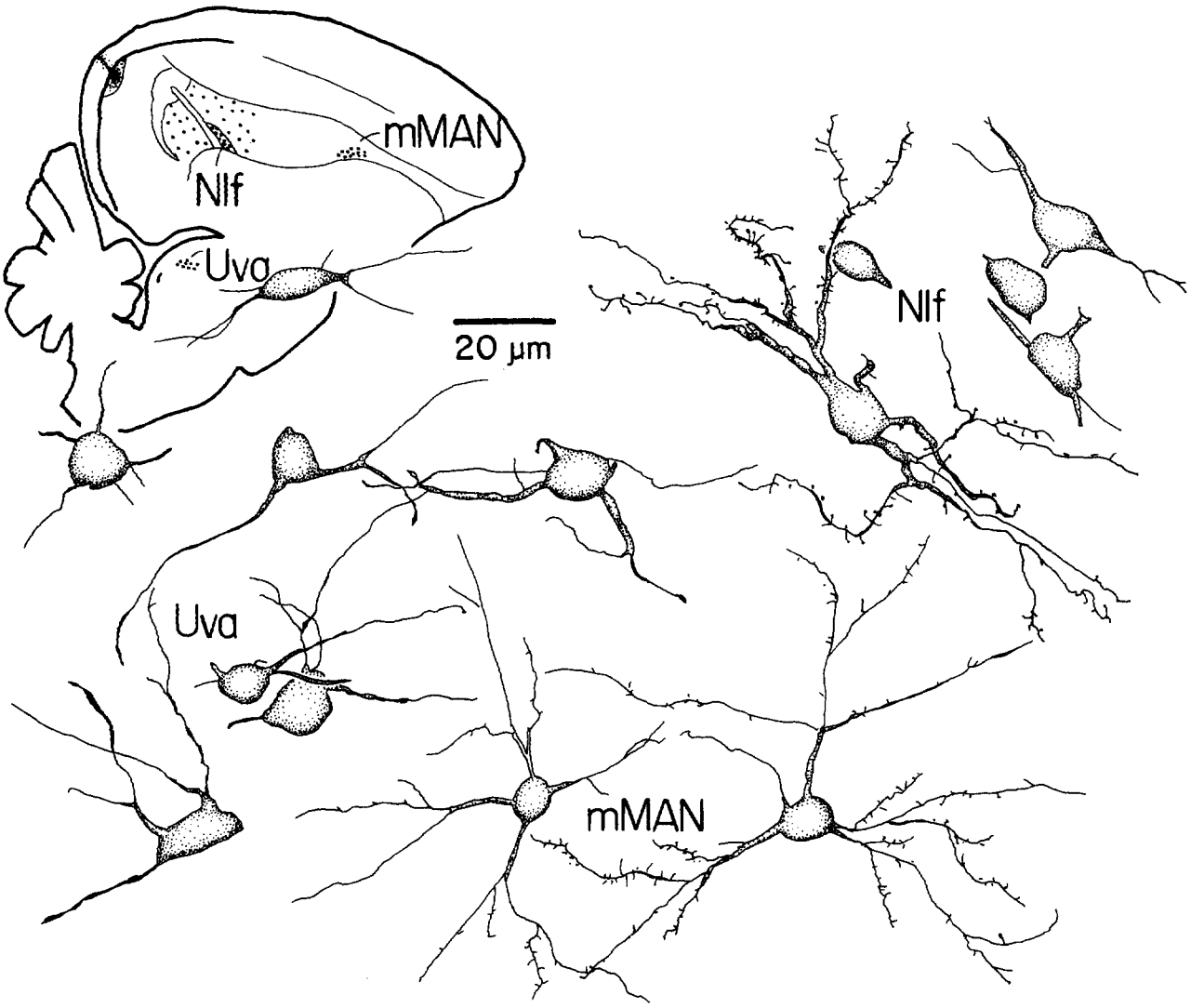

Fig. 20. Retrogradely labeled cells from injections into HVc. Dorsal is up and rostral is to the right. Top left is a schematic parasagittal section showing the pattern of retrograde labeling from injections into HVc. Surrounding this schematic are camera lucida drawings of cells in the respective nuclei (see Results). A photomicrograph of Uva cells is in Figure 22c.

caudomedial region is part of HVc (e.g., Nordeen et al., '87). We include the caudomedial region as a part of HVc because its border with the central subdivision of HVc is not distinct, it has all three morphological classes of cells found within HVc, the axons of cells in this region apparently ramify extensively within the other subdivisions of HVc, and the axons of cells in the other subdivisions of HVc apparently ramify extensively within the caudomedial region. Additionally, neurons in all three subdivisions project to both area X and RA. In all cases, area X-projecting cells appeared to be distributed evenly throughout HVc. Elucidation of the relative contributions of each of the subdivisions to the projection to area X, however, was not determined inthis study. RA-projecting cells were not as evenly distributed as area X-projecting cells, having a greater apparent density of cells and axons in dorsolateral HVc, and a lower density of cells in caudomedial HVc. Female HVc projects to area X but does not exhibit the subdivisions seen in the males. Male-like subdivisions are present in females treated with E2 early in life.

We find all three subdivisions in five other species (white-throated sparrows, eastern meadowlarks, western meadowlarks, indigo buntings, and canaries). The caudomedial 'small-celled' region has also been described in red-winged blackbirds (Kirn et al., '89), where HVc has a medial extension characterized by a high density of cells. On the basis of cytoarchitecture alone, Kirn et al. ('89) were unable to determine whether this medial region was part of HVc; however its shape and morphology is similar to the caudomedial region described in this report. Because similar subdivisions have been observed in seven passeriform species including distantly related species, the tripartite organization of HVc may obtain generally in male songbirds.

Superficially, HVc appears to have a simple structure but this appearance is misleading. The central region, which is the largest subdivision, has distinct boundaries in sections through the thickest part of HVc. Thus, most workers have shown one or a few low-power photomicrographs of HVc through its thickest part (e.g. Gurney, '81; Goldman and

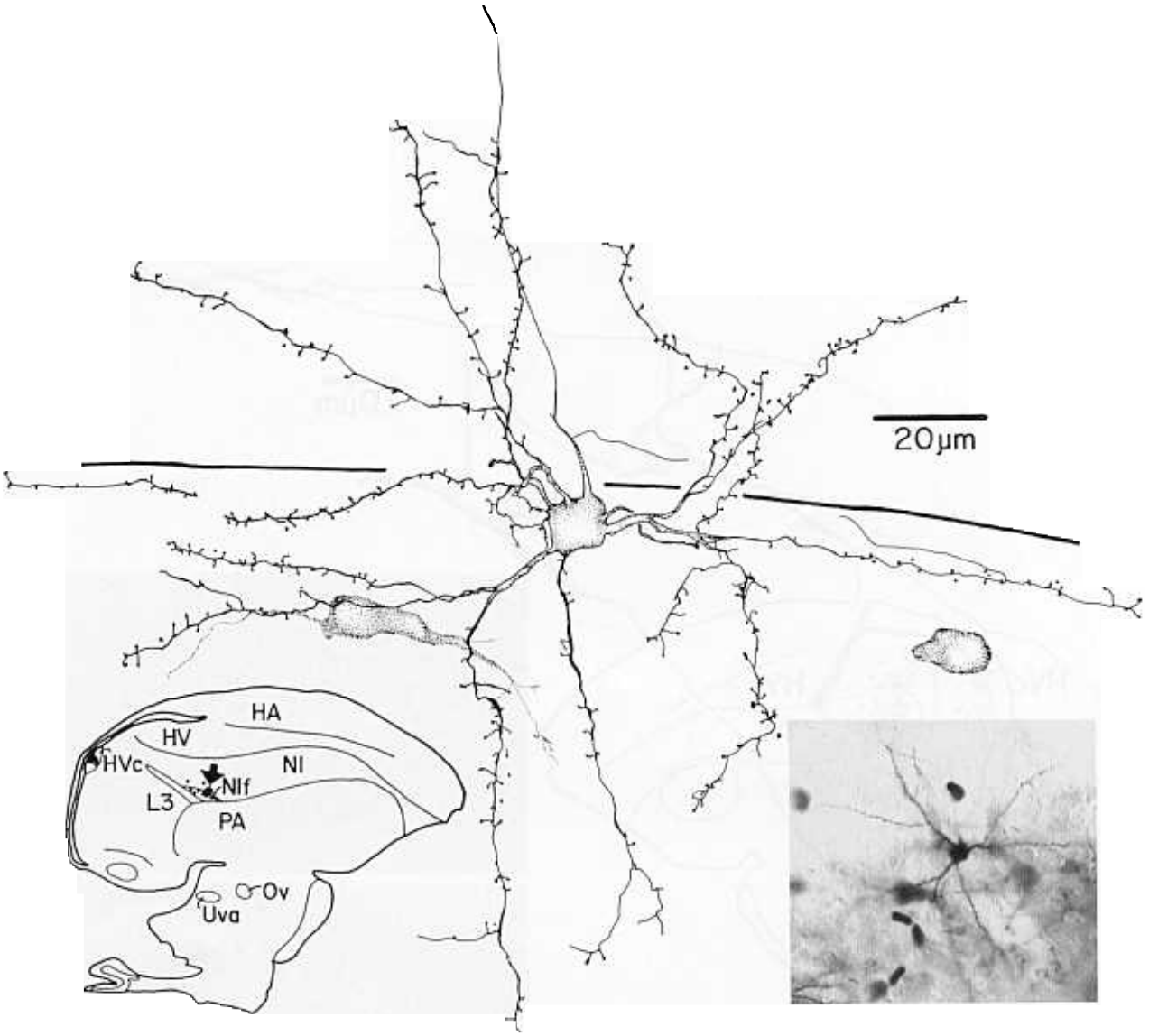

Fig. 21. Camera lucida drawing and photomicrograph of a retrogradely labeled cell in NIf from an injection into HVc. Case b03b. Dorsal is up and rostral is to the right. The dendrites of this cell extend into adjacent L1. **Inset** shows the location of the cell (arrow) and the injection site in the parasagittal section.

Nottebohm, '83; Margoliash, '83; Watson et al., '88; Bottjer et al., '89; Alvarez-Buylla et al., '90; Gahr, '90; Bernard et al., '93). This treatment implicitly defines HVc based solely on the cytoarchitectonic features of the central region. The definition of HVc based on the central region—a structure with large, darkly staining cells—is accurate for the central region but is incomplete because it excludes the small-celled caudomedial region. The caudomedial region and the dorsolateral zone are easily seen only in different planes of section, coronal and sagittal, respectively. In contrast, the central region is easily identified in both planes of section. because the central region has been used to define HVc, most workers have been satisfied with presenting data from only one plane of section. Also, the shelf does not cover the entire ventral border of HVc. The shelf is distinct along the ventral border of rostrolateral HVc but fades medially and fails to define the ventral border of the caudomedial region.

As a result of its misleading appearance, HVc's cytoarchitectonic features often have been treated cursorily. We identified over 100 studies involving HVc. Even in studies that are highly dependent on accurate cytoarchitectonic definitions, including numerous studies of HVc's volume and/or cytoarchitecture in relation to seasonal or hormonal changes or in relation to structure of song (e.g. syllable repertoire), the cytoarchitectonic definitions of HVc have typically been limited to a short phrase or have been absent altogether. In two studies, one of red-winged blackbirds (Kirn et al., '89) and the other of eastern meadowlarks (D. Margoliash, unpublished data), exclusion or inclusion of the volume of the caudomedial region did not change the statistical validity of the results. In another case, however, unanticipated seasonal changes in the cytoarchitecture of the caudomedial region may be the basis for seasonal changes in HVc's total volume (Nottebohm, '81; cf. Gahr,

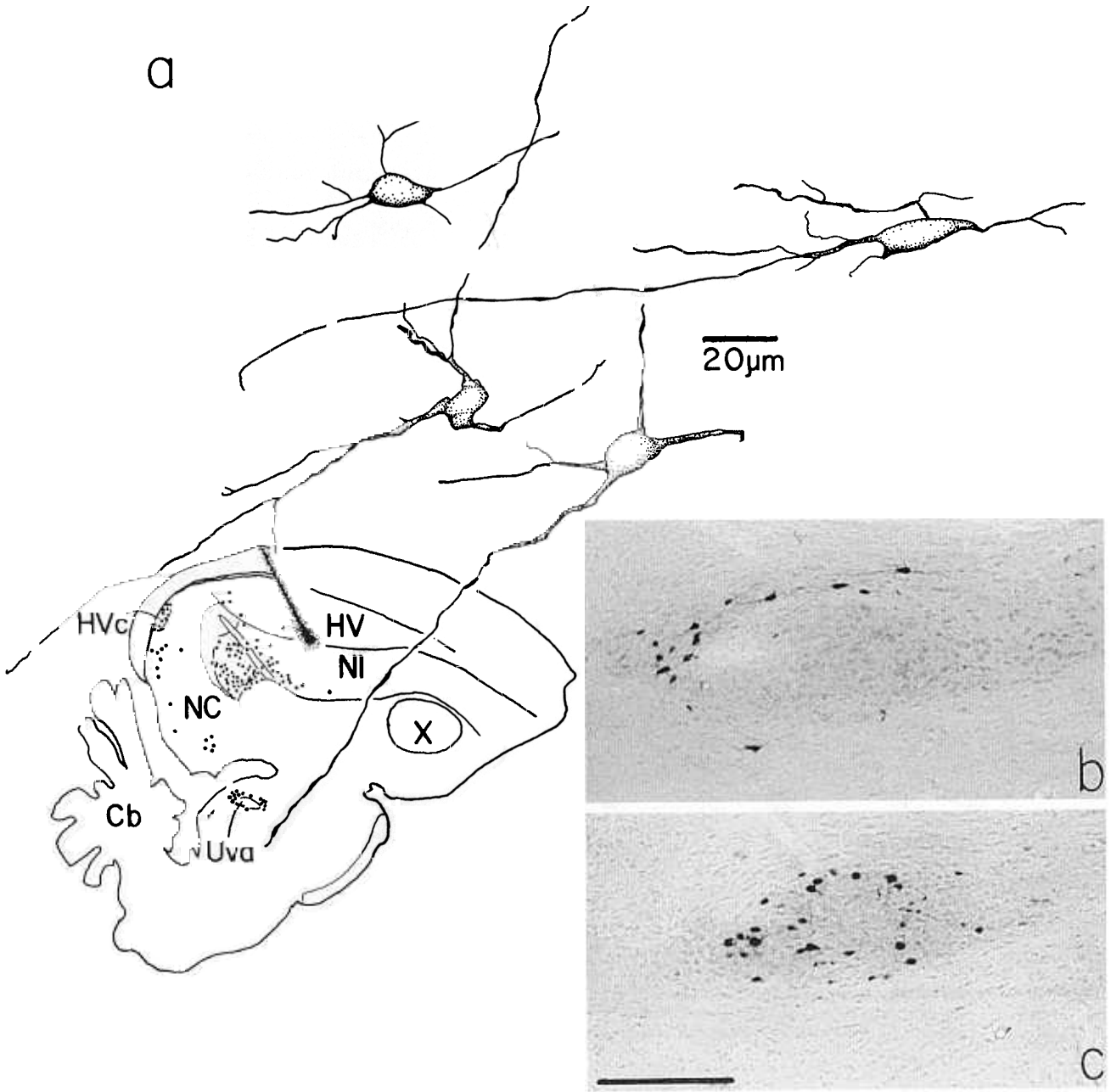

Fig. 22. **a:** Camera lucida drawing of retrogradely labeled cells near Uva from an injection into HV. Case b10a. Dorsal is up and rostral is to the right. **b:** Photomicrograph shows retrogradely labeled cells adjacent to Uva. Compare this with the photomicrograph (**c**) of labeled cells within Uva from an injection into HVc. Scale bar indicates 200 μm for b and c. **Inset** shows the injection into HV, and locations of retrogradely labeled cells throughout L1 and L3, HV, HVc, and in NC.

'90). In general, it will be necessary to re-examine results of studies based on incomplete descriptions of HVc. It will also be of interest to re-examine the distribution of various immunohistochemical markers and steroid hormone receptors localized to HVc (e.g., Arnold et al., '76; Watson et al., '88; Nordeen et al. '87; Gahr et al., '90; Braun et al., '91; Bernard et al., '93).

The shelf. This report establishes a cytoarchitectonic definition of the shelf that is not identical to previous definitions of the shelf. The original definition was based on the pattern of anterograde labeling from injections of tritiated amino acids into medial field L (Kelley and Nottebohm, '79). The shelf as defined by this technique is a region that circumscribes the medial and medioventral borders of HVc, but does not extend to the rostral and ventrolateral edges of HVc (see Fig. 3 of Kelley and Nottebohm, '79). The commonly used definition of the shelf, however, is based on cytoarchitecture: the shelf is the fiber rich zone along ventrolateral HVc that was originally thought to be LH (Kelley and Nottebohm, '79; see Nottebohm et al., '82). The shelf as described originally by Kelley and Nottebohm ('79) apparently overlaps both the caudomedial region of HVc and part of the cytoarchitectonically defined shelf. We have adopted the cytoarchitectonic defini-

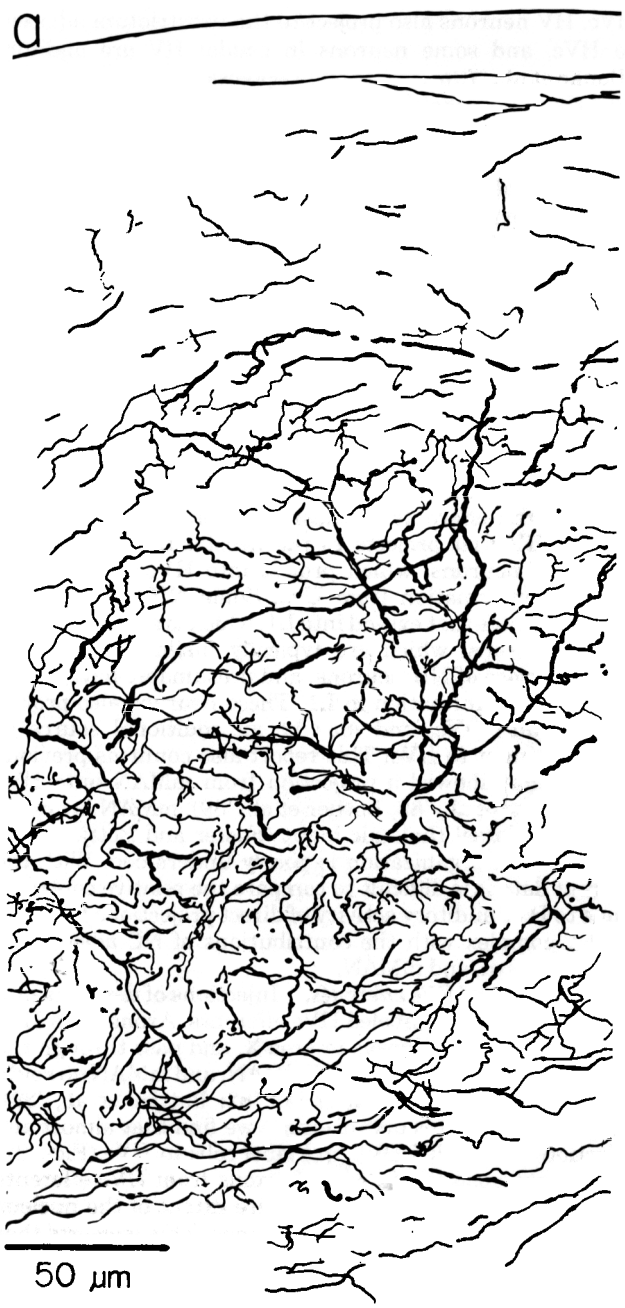

tion of the shelf for three reasons. First, because it is the most commonly used. Second, the shelf is clearly visible in a variety of histological material, including unstained sections viewed with Nomarski optics as well as in Nissl or fiber stained sections. Third, we have only occasionally reproduced the pattern of anterograde labeling from field L reported by Kelley and Nottebohm ('79).

Functional significance of HVc's connectivity

The present study can be interpreted in terms of the functional properties of HVc neurons. HVc has auditory neurons that are highly selective for the individual bird's autogenous (self-produced) song as compared to conspecific songs (Margoliash and Konishi, '85; Margoliash, '86). This selectivity results from song learning (Margoliash and Konishi, '85; Volman, '93; see Margoliash, '87), and derives from neuronal specificity for spectral and especially temporal parameters of autogenous song (Margoliash, '83; Margoliash and Fortune, '92). Elucidation of the neuronal circuits that give rise to these properties can give insight into the neural mechanisms of song learning, and into the organization of sensorimotor integration in the song system.

Projections of the field L complex to HVc. The sources of auditory input to HVc have been difficult to ascertain. Originally, it was reported that areas lateral to field L, but not field L itself, projected to HVc (Kelley and Nottebohm, '79). That study relied on an incomplete definition of field L, however, apparently including only the most medial regions of the field L complex but excluding the L1 and L3 subdivisions (see Fortune and Margoliash, '92a). Thus, the injections that Kelley and Nottebohm ('79) interpreted as being in field L were probably at the medial edge or medial to the field L complex. Those injections labeled an area ventral and medial to HVc, but not HVc itself. The finding by Katz and Gurney ('81) that ventral HVc neurons extend dendrites ventrally into the shelf and beyond provided a logic for auditory input to HVc, via the shelf (see also Margoliash, '87).

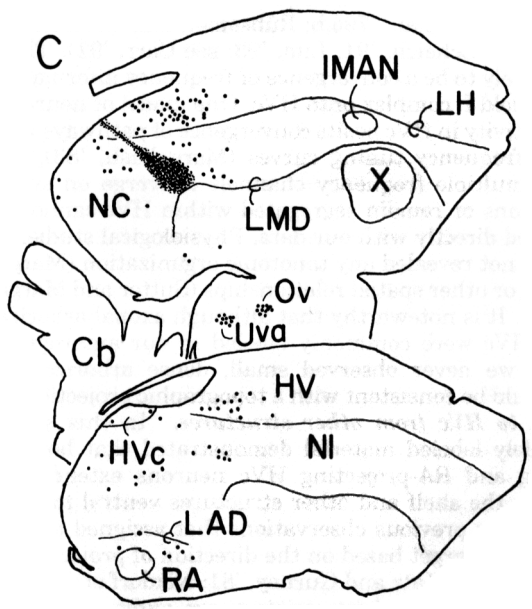

Fig. 23. Injection into the field L complex. Case b10a. **a:** Anterogradely and retrogradely labeled fibers in HVc. Dorsal is up and rostral is to the right. **b:** Box shows the location of **a**. Arrow in b indicates a group of labeled fibers ventral to HVc. **c:** The upper section shows the injection site; the lower section is that shown in a and b.

Injections lateral to what Kelley and Nottebohm ('79) considered to be field L anterogradely labeled HVc. When NIf was identified as an afferent of HVc (Nottebohm et al., '82), the anterograde labeling in HVc from Kelley and Nottebohm's ('79) lateral injection sites was interpreted to be labeling of the NIf pathway. Those lateral injections, however, were apparently situated primarily in L1 (compare Figure 10 of Kelley and Nottebohm, '79, with the data in Fortune and Margoliash, '92a). Subsequent studies using either Fink-Heimer degeneration or injections of horseradish peroxidase (HRP) also failed to demonstrate a direct projection from the field L complex (Kelley and Nottebohm, '79; Nottebohm et al., '82; Bottjer et al., '89). In over 20 injections of HVc at the beginning of this project using HRP as the retrograde tracer visualized according to a variety of published protocols (see Mesulam '82; Bottjer et al., '89), we found only a single retrogradely labeled cell in L1 (unpublished data) although cells in NIf, Uva, and in most cases mMAN, typically were well labeled.

In contrast to the HRP studies, in the present report injections of dextrans coupled to either biotin or fluorescent markers resulted in many labeled cells in the field L complex. The borders of injections of biotinylated dextrans, however, did not appear as discrete as HRP injection sites, and the injection sites were usually not as dark. For this reason we confirmed the extent of the injection site by localizing the region of cellular damage. In those cases where the injection site of biotinylated dextrans was distinct, the borders of the injection site corresponded to the area of cellular damage. It should also be noted that the massive convergence onto HVc results in a severe fibers-of-passage problem (L1, L2a, L3, NIf, Uva, NC, and HV project into and/or near to HVc); hence labeling in HVc after control injections of anterograde tracers into field L were not satisfying as confirmatory of the projection of field L to HVc. The definitive proof of field L's projection onto HVc will require intracellular labeling of individual cells.

We found retrogradely labeled cells from injections into HVc throughout L1 and L3 of the field L complex. Neurons in the field L complex that projected to HVc, therefore, are distributed throughout the frequency lamellae in the field L complex (Bonke et al., '79a,b; Rübsamen and Dörrscheidt, '86; Heil and Scheich, '91; Lim, '93; see Carr, '91). Thus, there is likely to be a convergence of frequency information from the field L complex onto HVc. One model of neuronal song selectivity in HVc posits convergence of pathways with different frequency tuning curves (Margoliash, '83), but whether multiple frequency channels converge on single HVc neurons or remain segregated within HVc cannot be determined directly with our data. Physiological studies of HVc have not revealed any tonotopic organization (Margoliash, '87) or other spatial relationships (Sutter and Margoliash, '94). It is noteworthy that although axonal arborizations in HVc were commonly labeled in our anterograde material, we never observed small, dense arborizations which would be consistent with a topographic projection.

Inputs to HVc from other structures. In this study, retrogradely labeled material demonstrated that both X-projecting and RA-projecting HVc neurons extend dendrites into the shelf and other structures ventral to HVc. This confirms previous observations that assigned to cells their efferent target based on the direction of projection of axon fragments (Katz and Gurney, '81; Nixdorf et al., '87). Neurons in the caudal neostriatum are auditory (Müller and Leppelsack, '85; Stripling et al., '94). L1 and L3, which project into HVc, also project to the neostriatum adjacent to HVc. HV neurons also project to the neostriatum adjacent to HVc, and some neurons in caudal HV are auditory (Bonke et al., '79b; Müller and Leppelsack, '85; Margoliash, '86; Heil and Scheich, '91). Thus, some ventral HVc neurons may receive HV and field L inputs, by way of dendrites that extend into the adjacent neostriatum. If this pathway is functionally important, it could impose a dorsoventral flow of information through HVc. In the only dorsoventral distinction of HVc physiology that we are aware of, Margoliash ('83) found more song-specific neurons in ventral than in dorsal HVc of the white-crowned sparrow (*Zonotrichia leucophrys*), although a sampling bias could not be excluded.

Auditory information can also enter HVc from multiple pathways. A recent report shows that there are auditory responses in Uva (Okuhata and Nottebohm, '92), which projects to HVc (Nottebohm et al., '82). Additionally, neurons adjacent to Uva project to HV. It is not known whether the efferents of these neurons overlap with the area of HV that projects to the neostriatum adjacent to HVc. NIf neurons, which project into HVc, may receive auditory information from Uva. Some NIf neurons also have dendrites that extend into L1, which is adjacent to NIf. These neurons, which are typically fusiform, may be a separate class of NIf neurons, and presumably have access to auditory information in L1. These neurons also project directly into HVc, and may be an additional source of auditory input to HVc. This report also confirms previous studies that showed a projection from mMAN onto HVc (Nottebohm et al., '82; Bottjer et al., '89). mMAN is known to receive dorsal thalamic input (Foster and Bottjer, '92); otherwise its organization is poorly understood. With the current data it is difficult to compare the relative contributions to HVc auditory activity of direct projections from the field L complex with the contributions of NC adjacent to HVc, NIf, Uva, and mMAN.

Divergence of HVc efferents. Injections of dextrans into HVc anterogradely labeled HVc efferents. Axons from HVc travel via many pathways to area X, and pass through the field L complex, HV, N, PA, PP, lMAN, and mMAN en route to area X (cf. Nottebohm et al., '82; Bottjer et al., '89). Consistent with this organization, we find that almost any injection into medial DVR will label cells in HVc (Figs. 22, 23; unpubl. results). In area X, axons from HVc efferents arborize broadly, covering the entire extent of the nucleus in both the sagittal and coronal planes. This suggests that many area X cells may receive input from a single HVc neuron. Because the arbors are broad and sparse, however, any single area X cell probably does not receive more than a few synapses from a single arbor.

In contrast, HVc efferents in RA form dense, branching arbors. Some fibers cross the entire nucleus, but most axons branch so much that it is difficult to determine the area over which they extend. Even our smallest injections into HVc produced dense labeling throughout RA, suggesting that the arbors have a broad extent. In contrast to area X cells, RA cells may each receive many synapses from a single HVc efferent. Herrmann and Arnold ('91), using published estimates of the number of neurons in RA, the volume of RA, and the density of synapses in RA, estimate that each RA neuron receives 650–800 synapses from HVc neurons, though the numbers of synapses from a single HVc efferent onto a single RA cell remains unknown.

Axons from HVc neurons arborize extensively within HVc. This was shown explicitly by Katz and Gurney ('81), who intracellularly labeled HVc neurons and described

their axon collaterals within HVc. The pattern of intrinsic projections remains unclear, however, both with respect to the morphological classes of HVc neurons and the subdivisions of HVc. In this study, many injections into HVc produced an uneven distribution of retrogradely labeled cells throughout the nucleus. There was, however, no consistent pattern of labeling in HVc between the various cases. This may be due to variations in the quality of staining or other histological factors, or this could be a result of idiosyncratic differences in the patterns of intrinsic connectivity. If the latter obtains, it could provide valuable insight into neuroanatomical correlates of song learning.

Summary. The broadly dispersed pattern of afferent termination within HVc, intrinsic HVc projections, and termination of HVc axons in RA and area X suggests the hypothesis of distributed representation of song at the level of HVc (Margoliash et al., '94). Recent physiological studies support this hypothesis. In urethane-anesthetized zebra finches, HVc responses to autogenous song at multiple recording sites demonstrated temporal synchrony but failed to find systematic spatial variation (Sutter and Margoliash, '94). Additionally, in chronic recordings from singing zebra finches, all HVc neurons were recruited for song. Typically, each neuron was active prior to and throughout the entire song (Yu and Margoliash, '92).

From these data we would predict changes in neural circuitry within HVc attendant to song learning are not limited to specific foci but are distributed across large parts of the nucleus.

Evolution of HVc

Our data demonstrate HVc in zebra finches has parallel inputs and outputs to the neostriatum adjacent to HVc (Fig. 24). HVc efferents terminate in RA and area X, and the efferents of NC adjacent to HVc terminate around RA and near to and/or in area X. Afferents from the field L complex terminate both in HVc and NC. Much of the NC data arise from control injections that were not fully investigated, and the organization of afferents and efferents in NC remain unclear. Nevertheless, the shared pattern of connectivity between HVc and adjacent NC suggests the possibility that these may structures share a common developmental and/or evolutionary origin.

There is a similar pattern of projections in other avian species, including the pigeon (*Columba livia*) and the budgerigar (*Melopsittacus undulatus*). In the pigeon, L1 and L3 cells project to dorsal caudal neostriatum. This region, in turn, projects to an area in medial archistriatum (Wild et al., '93). In the budgerigar field L projects to the ventrolateral intermediate neostriatum. Similarly, this region projects to an area in medial archistriatum (Brauth and McHale, '88). Because pigeons, budgerigars, and zebra finches are distantly related within birds, it is likely that this pattern of connections is a primitive feature of birds.

This suggests that during the evolution of oscine birds HVc may have emerged from a subdivision or duplication within NC that subsequently developed distinct cytoarchitectural features as it acquired increased functional specialization presumably related to auditory-feedback mediated song learning (Margoliash et al., '94). This hypothesis predicts that cytoarchitectonically indistinct subdivisions of NC in non-oscine birds will have similar patterns of connectivity as those described in this paper. Although a complete discussion is beyond the scope of this paper, such hypotheses can be tested by comparative analyses of other oscines and non-oscines chosen within a cladistic framework.

Nomenclature

HVc was identified as part of the ventral caudal hyperstriatum when the song system was first discovered and described in coronal sections in canaries (Nottebohm et al., '76). Recent data, however, suggest that HVc is a neostriatal nucleus (Nottebohm, '87), although final confirmation is lacking. In parasagittal sections HVc appears caudal to LH (which defines the caudal extent of HV), and appears to be part of dorsal caudal neostriatum (e.g., Fig. 4). The connectivity of HVc, including its relation to field L (auditory pathways) and its position relative to the somatosensory and visual pathways (see Margoliash et al., '94), is also consistent with a location in caudal neostriatum. Thus, the original designation of HVc was probably a misnomer, which has reasonably prompted attempts to rename the nucleus while retaining the acronym for consistency with the substantial previous literature. Whereas the suggested revisions 'higher (or high) vocal center' (e.g., Nottebohm, '87; Nottebohm et al., '90) has a similar acronym (HVC) it is nevertheless inadequate because of the implied functional attributes (hierarchical organization) and behavioral role. Although there is evidence for hierarchical organization in the song system (e.g., Doupe and Konishi, '91; Vu et al., '94), the hierarchical organization of the system may be viewed differently depending on the modality (esp. auditory vs. motor) and depending on the pathways under consideration (esp. the caudal pathway including RA vs. the rostral pathway including area X). What is meant by a "vocal" center is also unclear, which in any case may be an inappropriate term for potentially homologous forebrain structures in non-oscine species (Brenowitz, '91; Margoliash et al., '94). Because a proper anatomical name that

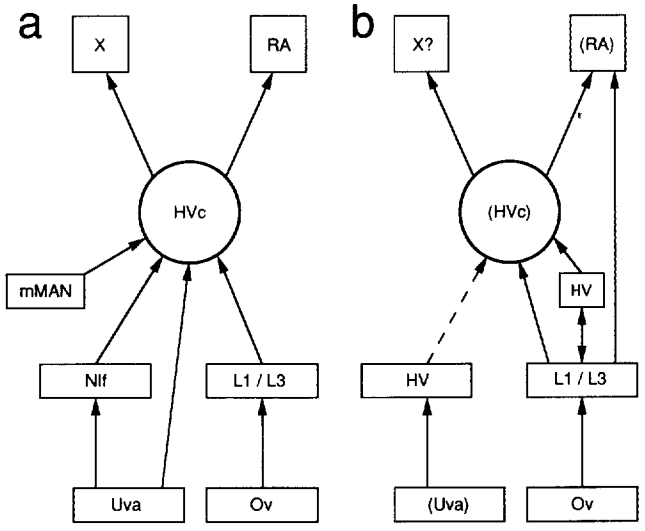

Fig. 24. Schematic summary of connections. **a:** Connections of HVc. **b:** Connections of the neostriatum adjacent to HVc. Parentheses indicate the area adjacent to the nucleus within the parentheses. The exact destination of (Uva) fibers in HV is not known. HV was shown to project onto the field L complex, though the specific subdivisions to which HV projects have not been conclusively identified. The dashed line indicates that the projection from (Uva) recipient HV to the area adjacent to HVc has not been demonstrated explicitly. It is not known whether the area adjacent to HVc projects directly into area X, around area X, or both.

retains the acronym is not possible, we have chosen to adopt the acronym itself as the proper name.

ACKNOWLEDGMENTS

We thank Mark Q. Martindale for use of microscopic and photographic equipment, and advice on the tracer techniques. Philip S. Ulinski advised us on histological techniques and provided a critical review of the manuscript. Masakazu Konishi generously loaned us prepared brains of female zebra finches treated with estrogen as juveniles. Clement Popovici provided technical assistance. This research was supported in part by the NIH (NS25677), the NSF (IBN-9309771), and the Whitehall Foundation (M91-03).

LITERATURE CITED

Alvarez-Buylla, A., J.R. Kirn, and F. Nottebohm (1990) Birth of projection neurons in adult avian brain may be related to perceptual or motor learning. Science *249:*1444–1446.

Alvarez-Buylla, A., C.Y. Ling, and F. Nottebohm (1992) High vocal center growth and its relation to neurogenesis, neuronal replacement and song acquisition in juvenile canaries. J. Neurobiol. *23:*396–406.

Arnold, A.P., F. Nottebohm, and D.W. Pfaff (1976) Hormone concentrating cells in vocal control and other areas of the brain of the zebra finch (*Poephila guttata*). J. Comp. Neurol. *165:*487–512.

Bernard, D.J., J.M. Casto, and G.F. Ball (1993) Sexual dimorphism in the volume of song control nuclei in European starlings: Assessment by a Nissl stain and autoradiography for muscarinic cholinergic receptors. J. Comp. Neurol. *334:*559–570.

Bonke, B.A., D. Bonke, and H. Scheich (1979a) Connectivity of the auditory forebrain nuclei in the guinea fowl (*Numida meleagris*). Cell Tissue Res. *200:*101–121.

Bonke, D., H. Scheich, and G. Langner (1979b) Responses of units in the auditory neostriatum of the guinea fowl (*Numida meleagris*) to species-specific calls and synthetic stimuli. I. Tonotopy and functional zones. J. Comp. Physiol. *132:*243–255.

Bottjer, S.W., S.L. Glaessner, and A.P. Arnold (1985) Ontogeny of brain nuclei controlling song learning and behavior in zebra finches. J. Neurosci. *5:*1556–1562.

Bottjer, S.W., K.A. Halsema, S.A. Brown, and E.I. Miesner (1989) Axonal connections of a forebrain nucleus involved with vocal learning in zebra finches. J. Comp. Neurol. *279:*312–326.

Braun, K., and H. Scheich (1988) Physiological bases of the development of behavior. Verh. Dtsch. Zool. Ges. *81:*77–95.

Braun, K., H. Scheich, C.W. Heizmann, and W. Hunziker (1991) Parvalbumin and calbindin-D28K immunoreactivity as developmental markers of auditory and vocal motor nuclei of the zebra finch. Neuroscience *40:*853–869.

Brauth, S.E., and C.M. McHale (1988) Auditory pathways in the budgerigar. II. Intratelencephalic pathways. Brain Behav. Evol. *32:*193–207.

Brenowitz, E.A. (1991) Evolution of the vocal control system in the avian brain. Neurosciences *3:*399–407.

Brenowitz, E.A., and A.P. Arnold (1986) Interspecific comparisons of the size of neural song control regions and song complexity in duetting birds: Evolutionary implications. J. Neurosci. *6:*2875–2879.

Canady, R.A., D.E. Kroodsma, and F. Nottebohm (1984) Population differences in complexity of a learned skill are correlated with the brain space involved. Proc. Natl. Acad. Sci. USA *81:*6232–6234.

Carr, C.E. (1991) Central auditory pathways of reptiles and birds. In D.B. Webster, R.R. Fay, and A.N. Popper (eds.): The Evolutionary Biology of Hearing. New York: Springer-Verlag.

DeVoogd, T.J., J.R. Krebs, S.D. Healy, and A. Purvis (1993) Relations between song repertoire size and the volume of brain nuclei related to song: Comparative evolutionary analyses amongst oscine birds. Proc. R. Soc. Lond. [Biol.] *254:*75–82.

Doupe, A.J., and M. Konishi (1991) Song-selective auditory circuits in the vocal control system of the zebra finch. Proc. Natl. Acad. Sci. USA *88:*11339–11343.

Durand, S.E., J.M. Tepper, and M.-F. Cheng (1992) The shell region of the nucleus ovoidalis: A subdivision of the avian auditory thalamus. J. Comp. Neurol. *323:*495–518.

Fortune, E.S., and D. Margoliash (1991) Thalamic input and cytoarchitecture of auditory neostriatum in zebra finch. Soc. Neurosci. Abstr. *17:*446.

Fortune, E.S., and D. Margoliash (1992a) Cytoarchitectonic organization and morphology of cells of the field L complex in male zebra finches (*Taeniopygia guttata*). J. Comp. Neurol. *325:*388–404.

Fortune, E.S., and D. Margoliash (1992b) Neurons in the field L complex of the male zebra finch project directly into HVc. Proc. Third Int. Cong. Neuroethol. 345.

Fortune, E.S., and D. Margoliash (1992c) Multiple auditory pathways into HVc. Soc. Neurosci. Abstr. *18:*500.

Fortune, E.S., and D. Margoliash (1994) In vivo characterization of identified HVc neurons in the zebra finch. Soc. Neurosci. Abstr. *20:*165.

Foster, E.F., and S.W. Bottjer (1992) Axonal connections of a forebrain nucleus in male zebra finches. Soc. Neurosci. Abstr. *18:*528.

Gahr, M. (1990) Delineation of a brain nucleus: Comparisons of cytochemical, hodological, and cytoarchitectural views of the song control nucleus HVC of the adult canary. J. Comp. Neurol. *294:*30–36.

Gamlin, P.D.R., and D.H. Cohen (1986) A second ascending visual pathway from the optic tectum to the telencephalon in the pigeon (*Columba livia*). J. Comp. Neurol. *250:*296–310.

Goldman, S.A., and F. Nottebohm (1983) Neuronal production, migration, and differentiation in a vocal control nucleus of the adult female canary brain. Proc. Natl. Acad. Sci. USA *80:*2390–2394.

Gurney, M. (1981) Hormonal control of cell form and number in the zebra finch song system. J. Neurosci. *1:*658–673.

Heil, P., and H. Scheich (1991) Functional organization of the avian auditory cortex analogue. I. Topographic representation of isointensity bandwidth. Brain Res. *539:*110–120.

Herrmann, K., and A.P. Arnold (1991) The development of afferent projections to the robust archistriatal nucleus in male zebra finches: A quantitative electron microscopic study. J. Neurosci. *11:*2063–2074.

Johnson, F., and S.W. Bottjer (1993) Hormone-induced changes in identified cell populations of the higher vocal center in male canaries. J. Neurobiol. *24:*400–418.

Karten, H.J. (1967) The organization of the avian ascending auditory pathway in the pigeon (*Columba livia*). I. Diencephalic projections of the inferior colliculus (Nucleus mesencephalicus lateralis, pars dorsalis). Brain Res. *6:*409–427.

Karten, H.J. (1968) The ascending auditory pathway in the pigeon (*Columba livia*). II. Telencephalic projections of the nucleus ovoidalis thalami. Brain Res. *11:*134–153.

Katz, L.C., and M.E. Gurney (1981) Auditory responses in the zebra finch's motor system for song. Brain Res. *211:*192–197.

Kelley, D.B., and F. Nottebohm (1979) Projections of a telencephalic auditory nucleus—Field L—in the canary. J. Comp. Neurol. *183:*455–470.

Kirn, J.R., R.P. Clower, D.E. Kroodsma, and T.J. DeVoogd (1989) Song-related brain regions in the red-winged blackbird are affected by sex and season but not repertoire size. J. Neurobiol. *20:*139–163.

Kirn, J.R., A. Alvarez-Buylla, and F. Nottebohm (1991) Production and survival of projection neurons in a forebrain vocal center of adult male canaries. J. Neurosci. *11:*1756–1762.

Korzeniewska, E., and O. Güntürkün (1990) Sensory properties and afferents of the N. dorsolateralis posterior thalami of the pigeon. J. Comp. Neurol. *292:*457–479.

Lim, D. (1993) Auditory response properties of field L in the zebra finch. Soc. Neurosci. Abstr. *19:*415.

Margoliash, D. (1983) Acoustic parameters underlying the responses of song-specific neurons in the white-crowned sparrow. J. Neurosci. *3:*1039–1057.

Margoliash, D. (1986) Preference for autogenous song by auditory neurons in a song system nucleus of the white-crowned sparrow. J. Neurosci. *6:*1643–1661.

Margoliash, D. (1987) Neural plasticity in birdsong learning. In J.P. Rauschecker and P. Marler (eds): Imprinting and Cortical Plasticity. New York: John Wiley and Sons.

Margoliash, D., and E.S. Fortune (1992) Temporal and harmonic combination-sensitive neurons in the zebra finch's HVc. J. Neurosci. *12:*4309–4326.

Margoliash, D., and M. Konishi (1985) Auditory representation of autogenous song in the song-system of white-crowned sparrows. Proc. Natl. Acad. Sci. USA *82:*5997–6000.

Margoliash, D., E.S. Fortune, M.L. Sutter, A.C. Yu, and B.D. Wren-Hardin (1994) Distributed representation in the oscine song system: Functional and evolutionary implications. Brain Behav. Evol. *44:*247–264.

Mesulam, M.M. (1982) Tracing neural connections with horseradish peroxidase. New York: John Wiley & Sons, Inc.

Müller, C.M., and H-J. Leppelsack (1985) Feature extraction and tonotopic organization in the avian auditory forebrain. Exp. Brain Res. *59:*587–599.

Nordeen, K.W., E.J. Nordeen, and A.P. Arnold (1987) Estrogen accumulation in zebra finch song control nuclei: Implications for sexual differentiation and adult activation of song behavior. J. Neurobiol. *18:*569–582.

Nottebohm, F. (1981) A brain for all seasons: Cyclical anatomical changes in song-control nuclei of the canary brain. Science *214:*1368–1370.

Nottebohm, F. (1987) Birdsong. In G. Adelman (ed): Encyclopedia of Neuroscience. Boston: Birkhäuser.

Nottebohm, F., T.M. Stokes, and C.M. Leonard (1976) Central control of song in the canary, *Serinus canarius.* J. Comp. Neurol. *165:*457–486.

Nottebohm, F., S. Kasparian, and C. Pandazis (1981) Brain space for a learned task. Brain Res. *213:*99–109.

Nottebohm, F., D.B. Kelley, and J.A. Paton (1982) Connections of vocal control nuclei in the canary telencephalon. J. Comp. Neurol. *207:*344–357.

Nottebohm, F., M.E. Nottebohm, and L. Crane (1986) Developmental and seasonal changes in canary song and their relation to changes in the anatomy of song-control nuclei. Behav. Neural Biol. *46:*445–471.

Nixdorf, B.E., S.S. Davis, and T.J. DeVoogd (1989) Morphology of Golgi-impregnated neurons in hyperstriatum ventralis, pars caudalis in adult male and female canaries. J. Comp. Neurol. *284:*337–349.

Nottebohm, F., A. Alvarez-Buylla, J. Cynx, J. Kirn, C.-Y. Ling, M. Nottebohm, R. Suter, A. Tolles, and H. Williams (1990) Song learning in birds: the relation between perception and production. Philos. Trans. R. Soc. Lond. [Biol]. *329:*115–124.

Okuhata, S., and F. Nottebohm (1992) Single units in nucleus UVA respond to sound and respiration and are part of a motor loop in song production. Proc. Third Int. Cong. Neuroethol. 60.

Rübsamen, R., and G.J. Dörrscheidt (1986) Tonotopic organization of the auditory forebrain in a songbird, the European starling. J. Comp. Physiol. [A] *158:*639–646.

Saini, K.D., and H.-J. Leppelsack (1981) Cell types of the auditory caudomedial neostriatum of the starling (*Sturnus vulgaris*). J. Comp. Neurol. *198:*209–229.

Stripling, R., S.F. Volman, and D.F. Clayton (1994) Electrophysiological responses to song presentation in caudomedial neostriatum of zebra finches: Links to ZENK gene induction. Soc. Neurosci. Abstr. *20:*165.

Sutter, M.L., and D.L. Margoliash (1994) Global synchronous response to autogenous song in zebra finch HVc. J. Neurophysiol. *72:*2105–2123.

Vicario, D.S., and K.H. Yohay (1993) Song-selective auditory input to a forebrain vocal control nucleus in the zebra finch. J. Neurobiol. *24:*488–505.

Volman, S.F. (1993) Development of neural selectivity for song during vocal learning. J. Neurosci. *13:*4737–4747.

Vu, E.T., M.E. Mazurek, and Y.-C. Kuo (1994) Identification of a forebrain motor programming network for the learned song of zebra finches. J. Neurosci. *14:*6924–6934.

Watson, J.T., E. Adkins-Regan, P. Whiting, J.M. Lindstrom, and T.R. Podleski (1988) Autoradiographic localization of nicotinic acetylcholine receptors in the brain of the zebra finch (*Peophila guttata*). J. Comp. Neurol. *274:*255–264.

Wild, J.M. (1993) Does the pigeon have a nucleus uvaeformis (Uva), or the songbird a nucleus dorsolateralis posterior thalami, pars caudalis (cDLP)? Soc. Neurosci. Abstr. *19:*415.

Wild, J.M., H.J. Karten, and B.J. Frost (1993) Connections of the auditory forebrain in the pigeon (*Columba livia*). J. Comp. Neurol. *337:*32–62.

Yu, C.-H., and D. Margoliash (1992) Recording of HVc in singing zebra finches. Proc. Third Int. Cong. Neuroethol. 342.